*Catalysts* **2013**, *3*, 36-73; doi:10.3390/catal3010036

OPEN ACCESS

*catalysts*

**ISSN 2073-4344**

www.mdpi.com/journal/catalysts

*Review*

# Brookite, the Least Known $TiO_2$ Photocatalyst

**Agatino Di Paola *, Marianna Bellardita and Leonardo Palmisano**

"Schiavello-Grillone" Photocatalysis Group, Dipartimento di Energia, Ingegneria dell'Informazione, e modelli Matematici (DEIM), Università di Palermo, Viale delle Scienze, 90128 Palermo, Italy; E-Mails: marianna.bellardita@unipa.it (M.B); leonardo.palmisano@unipa.it (L.P.)

* Author to whom correspondence should be addressed; E-Mail: agatino.dipaola@unipa.it; Tel.: +39-091-238-63729; Fax: +39-091-702-5020.

*Received: 12 November 2012; in revised form: 9 January 2013 / Accepted: 10 January 2013 / Published: 18 January 2013*

---

**Abstract:** Brookite is the least studied $TiO_2$ photocatalyst due to the difficulties usually encountered in order to obtain it as a pure phase. In this review, a comprehensive survey of the different methods available for preparing brookite powders and films is reported. Attention has been paid both to the most traditional methods, such as hydrothermal processes at high temperatures and pressures, and to environmentally benign syntheses using water soluble compounds and water as the solvent. Papers reporting the photocatalytic activity of pure and brookite-based samples have been reviewed.

**Keywords:** $TiO_2$; brookite; brookite nanostructures; brookite films; mixtures of $TiO_2$ phases; brookite-based photocatalysts

---

## 1. Introduction

Titanium dioxide ($TiO_2$) has attracted considerable attention for various applications such as pigments, photocatalysis, dye-sensitized solar cells, sensor devices, cosmetics and protective coatings. In particular, $TiO_2$ is the most studied photocatalyst because of its high efficiency, non-toxicity, chemical and biological stability, and low cost.

$TiO_2$ exists mainly in three different crystalline habits: rutile (tetragonal), anatase (tetragonal) and brookite (orthorombic). Rutile is the stable form, whereas anatase and brookite are metastable and are readily transformed to rutile when heated. Anatase is the phase normally found in the sol-gel syntheses of $TiO_2$ but brookite is often observed as a by-product when the precipitation is carried out in an acidic

medium at low temperature. Pure brookite without rutile or anatase is rather difficult to be prepared so that, until recently, its photocatalytic properties have been not much studied.

In recent years, the interest in brookite has increased and pure brookite has demonstrated to be an interesting candidate in photocatalytic applications. As illustrated in Figure 1, the number of papers on the preparation and photocatalytic activity of pure brookite and brookite-based samples is undergoing an exponential increase and the rate of publication shows no declining signs. Most of the papers on brookite simply concern its preparation.

**Figure 1.** Published papers on the topic of brookite. Source: ISI Web of Knowledge database. Consulted: 4 October 2012.

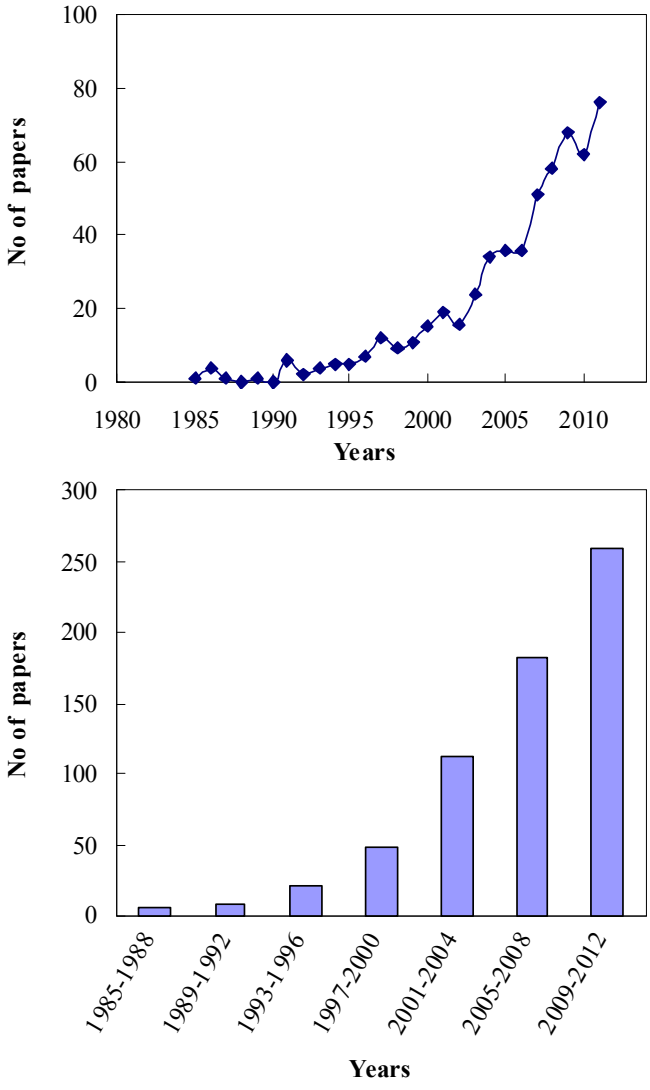


This review gives an overview, as complete and updated as possible, of the preparation and characterization of brookite and brookite-based photocatalysts that have been tested for environmental remediation, hydrogen formation, Li ion batteries and organic syntheses. A short section has been reserved to doped brookite materials that are increasingly studied as possible visible light-responsive photocatalysts.

## 2. Brookite

### *2.1. Characterization*

Brookite has an orthorhombic crystalline structure with a unit cell described by the space group *Pbca* [1]. The structure is composed of octahedra, each with a titanium atom at its center and oxygen atoms at its corners (Figure 2). The octahedra share edges and corners with each other to such an extent as to give the crystal the correct chemical composition. The octahedra are distorted and present the oxygen atoms in two different positions [2]. The bond lengths between the titanium and oxygen atoms are all different.

**Figure 2.** Representative octahedron of the crystalline structure of brookite [2].

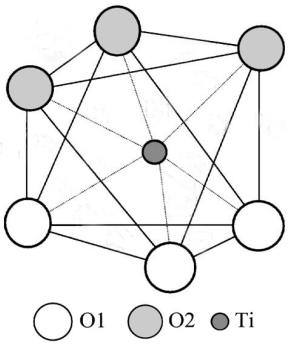


Oxygen atoms in the octahedron are distributed on the two faces nearly perpendicular to the (100) direction [2]. One face has oxygen atoms of type O1; the other one, oxygen atoms of type O2. Every octahedron shares three edges: one of them determines the crystal distribution along the (100) direction, and the other two determine it along the (001) direction (see Figure 3).

**Figure 3.** Crystalline structure of brookite [2].

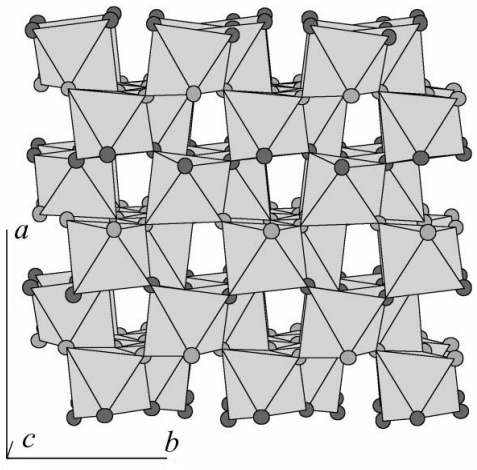


Octahedra arrangement produces a crystalline structure with tunnels along the c-axis, in which small cations like hydrogen or lithium can be incorporated.

X-ray diffraction (XRD) analysis is usually used to prove the presence of brookite in a sample. As shown in Figure 4, the existence of brookite in the XRD patterns is clearly evidenced from the

presence of the (121) peak at 2θ = 30.81°. Anyway, for the interpretation of the diffractograms it is necessary to take into account that the main (101) diffraction peak of anatase at 2θ = 25.28° overlaps with the (120) and (111) peaks of brookite at 2θ = 25.34° and 25.69°, respectively, so that apparently pure brookite samples can be a mixture of anatase and brookite.

**Figure 4.** X-ray diffraction (XRD) analysis patterns of anatase and brookite.

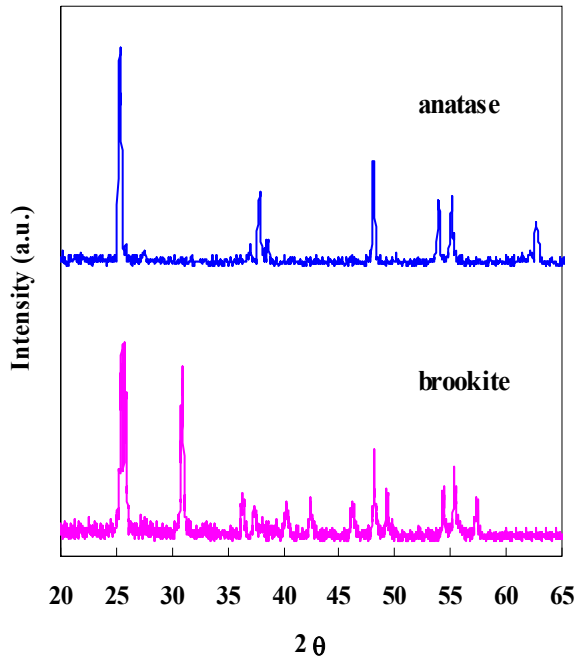


Ideal brookite has a $I^{(121)}_{brookite}/I^{(120)}_{brookite}$ ratio of ~0.9 (JCPDS No. 29-1360) but many of the claimed pure brookite powders reported in literature show $I^{(121)}_{brookite}/I^{(120)}_{brookite}$ ratios significantly lower than this value [3]. This does not imply necessarily the presence of anatase since samples synthesized at low temperatures are often scarcely crystalline and the corrected ratio could be easily reached by calcination at relatively high temperatures. On the other hand, an unusual single (121) peak was found for a film containing neither anatase nor rutile obtained by a modified sol–gel method [4]. Hu *et al.* [5] used one characteristic peak of anatase at 2θ = 62.57°, which does not overlap with any diffraction peak of brookite, to ascertain the existence of anatase.

According to Bokhimi and Pedraza [6] the only way to prove that the samples are single brookite phase is to run their XRD patterns with a good statistic to refine the crystalline structure of brookite in order to demonstrate that the modeling of only this phase is enough to reproduce the experimental diffraction pattern. The Rietveld refinement method has been often applied considering the whole pattern and not only the single peaks [7].

Raman spectroscopy is a very sensitive tool to confirm the existence of only brookite in a sample since brookite is characterized by a relatively complex vibrational spectrum when compared with the other $TiO_2$ polymorphs [8]. As shown in Figure 5, the overall spectral profile of brookite is characterized by a very strong band at 153 $cm^{-1}$ and a grouping of weaker, higher wavenumber bands. In comparison, the vibrational spectrum of anatase is relatively simple in accord with its greater crystal symmetry. The absence of the characteristic peak at 516 $cm^{-1}$ allows for exclusion of the presence of anatase in the samples.

**Figure 5.** Raman spectra of brookite and anatase.

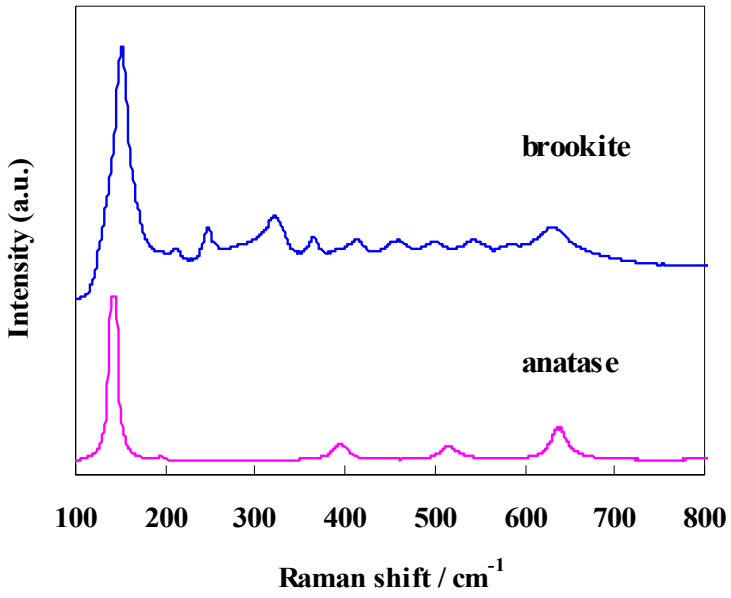


By calcination at high temperatures, brookite is transformed to rutile. The transformation occurs directly or via anatase depending on several factors including crystallite size, size distribution and contact area of the crystallites in the powder. Zhang and Banfield [9] found a correlation among the surface enthalpies of the three polymorphs and their particle size. The energies of anatase, brookite and rutile are sufficiently close that they can be reversed by small differences in surface energies. Brookite is more stable than anatase for crystal sizes greater than 11 nm while rutile is the most stable phase at sizes greater than 35 nm. Zhu *et al.* [10] developed an empirical expression on a critical grain size of brookite, $D_c$, which dominates the transition sequence between anatase and brookite. When the size of brookite $D_b$ is larger than $D_c$, brookite directly transforms to rutile whereas, when $D_b$ is smaller than $D_c$, brookite transforms to anatase and then anatase to rutile.

### *2.2. Electronic Properties*

The knowledge of the electronic band structure of the $TiO_2$ polymorphs is useful to understand the photocatalytic behaviour of the pure phases and of their mixtures. Theoretical and experimental works report band gap values for brookite both smaller and larger than that of anatase. In 1985, Grätzel and Rotzinger [11] were the first to estimate the band gap value, $E_g$, of brookite as 3.14 eV by extended Hückel molecular orbital calculations. The $E_g$, was intermediate between those of anatase (3.23 eV) and rutile (3.02 eV). Mo and Ching [12] used the self-consistent orthogonalized linear combination of atomic orbitals method to study the electronic structure and the optical properties of anatase, brookite and rutile. According to their calculations, brookite had a direct band gap of 2.20 eV, which is larger than that of anatase and rutile (1.78 eV for rutile and 2.04 eV for anatase, respectively). These results, as reported by the same authors, were an underestimation of the effective band gap values. Park *et al.* [13] calculated an $E_g$ value of 2.1 eV for brookite using the Kohn-Sham method, which underestimates systematically the band gap often by more than 50%. Recently, standard density functional theory calculations [14] showed that brookite and rutile had a direct band gaps of 1.86 eV and 1.88 eV, respectively, whereas an indirect band gap of 1.94 eV was observed for anatase. Using a more modern

approximation, the band gap underestimation was corrected and the $E_g$ values of brookite, rutile and anatase were increased to 3.30 eV, 3.39 eV and 3.60 eV [14].

Experimental band gap energies ranging from 3.1 to 3.4 eV have been reported for brookite, but there is disagreement on whether the optical response is attributable to direct or indirect transitions. The band gap was usually determined by diffuse reflectance measurements, from the tangent lines to the plots of the modified Kubelka-Munk function, $[F(R'_\infty)h\nu]^{1/2}$, *versus* the energy of the exciting light [15] considering brookite as an indirect semiconductor [16–24]. Direct band gap values have been also obtained [3,5,16,17,25].

The precise value of $E_g$ is currently unknown since the experimental results often refer to samples not well crystallized. Zallen and Moret [26] reported that natural crystals of brookite had an indirect band gap of about 1.9 eV. This low value is ascribable to the presence of impurities in the mineral that was pale brown in color. On the other hand, different band gap values were obtained by varying the duration of the hydrothermal treatment [18] or the kind of nanostructure (nanosheets, nanospindles, nanoflowers) [27]. Koelsch *et al.* [21] determined the band gap of brookite nanoparticles as 3.4 eV, measuring the optical transmission of brookite dispersions at different concentrations and by UV fluorescence measurements. Shibata *et al.* [28] photoelectrochemically determined a band gap value of 3.26 eV for films consisting mostly of brookite phase with some anatase. A value of 3.29 eV was obtained by crystallization at 450 °C of a sample of brookite prepared by thermohydrolysis of $TiCl_4$ at 100 °C [24]. This value compares well with the value of 3.31 eV found for brookite nanorods [23].

The flatband potential, ($E_{FB}$), of a semiconductor is a fundamental property for the thermodynamics of the interfacial electron transfer steps. For an n-type semiconductor as $TiO_2$ it can be assumed that the positions of the flatband potential and the quasi-Fermi level ($^*E_f$) are the same and very close to the lower edge of the conduction band [29].

Grätzel and Rotzinger [11] firstly reported a rough estimate of $E_{FB} = -0.03$ V *vs.* NHE for brookite based on a theoretical band gap value of 3.14 eV. Di Paola *et al.* [30] determined the flat band potentials of anatase, brookite, and rutile by a slurry method [31] measuring the photovoltage of the corresponding suspensions in the presence of methylviologen dichloride as a function of pH. As shown in Figure 6, the values obtained at pH 7 were −0.45 V for anatase, −0.46 V for brookite, and −0.37 V for rutile. It is worth noting that the experimental $E_{FB}$ value found for brookite is practically coincident with that calculated theoretically (−0.44 V at pH 7 [11]).

Kandiel *et al.* [23] calculated the flat-band potentials of anatase and brookite by impedance spectroscopy using electrodes obtained by spreading the corresponding suspensions on conductive fluorine-tin oxide glasses. The quasi-Fermi levels ($^*E_f$) were, furthermore, obtained under UV illumination by the slurry method. The $E_{FB}$ values estimated at pH 7 *versus* NHE were −0.35 V for anatase and –0.54 V for brookite whereas the corresponding $^*E_f$ values were −0.68 V and −0.77 V. The differences between these values were attributed to the independent methods performed under dark and illuminated conditions. The conduction band edges of anatase and brookite were calculated as the mean value of $E_{FB}$ and $^*E_f$, *i.e.*, −0.51 V for anatase and −0.65 V for brookite.

**Figure 6.** Electrochemical potentials of the band edges of anatase, brookite, and rutile at pH = 7 [30].

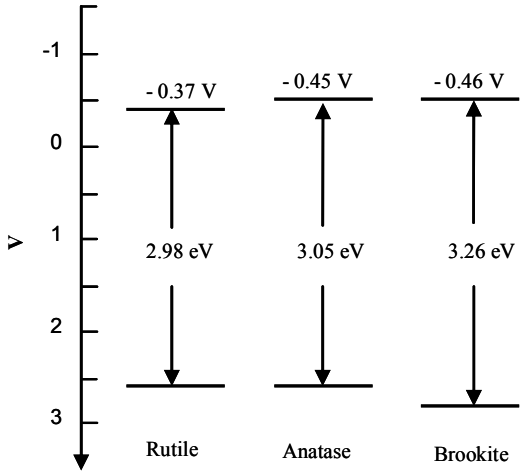


Recently, Truong *et al.* [32] reported values of −0.91 V and −0.96 V *vs.* NHE at pH 7 for the conduction band edges of anatase and brookite, respectively, without citing the methods used to determine them.

The few experimental values of flat band potential of brookite reported in literature and the uncertainty on its band gap do not allow to exactly locate the position of the conduction and valence band edges of the three oxides of titanium. Anyway, the most probable hypothesis is that the flat band of brookite is shifted negatively with respect to that of anatase.

## 3. Brookite Preparation

### *3.1. Pure Brookite Powders*

The first works on the synthesis of brookite date back to the late 1950s. Classically, brookite was synthesized from titanium(IV) compounds in aqueous or organic media by hydrothermal methods at high temperatures and pressures. Mixtures of anatase and brookite were prepared by thermal treatment of the amorphous $TiO_2$ powders obtained by hydrolysis of titanium(IV) tetraethoxide [33–35]. Yamaguchi found that a film of brookite was obtained on the surface of a Ti foil by anodization in a solution of $H_2SO_4$ (50% by weight) [36]. Complete transformation of anatase to brookite was achieved by grinding for 30 h samples previously heated for several hours to 600 °C [37] or anatase-brookite mixtures obtained by hydrolysis of titanium alcolate [38].

Keesmann [39] was the first to synthesize pure brookite by hydrothermal treatment of amorphous $TiO_2$ obtained by hydrolysis of titanium tetraisopropoxide or alkaline titanates, in the presence of a solution of NaOH containing 3–25 atoms % of Na with respect to (Ti + Na). $Na^+$ ions were considered to stabilize the lattice of brookite but Schwarzmann and Ognibeni [40] obtained well crystallized brookite by hydrothermal treatment of $TiO_2 \cdot xH_2O$ between 100 and 300 °C in the absence of $Na^+$ ions.

Basic environments are not essential for the formation of brookite and this phase was also prepared by oxidation of an aqueous acidic $TiCl_3$ solution containing $CH_3COONa$ under a flux of air at 95 °C [41,42]. Moreover, brookite was synthesized by hydrothermal oxidation of Ti metal in a NaF

solution at 200–500 °C [43]. It was also formed from systems containing $TiH_2$ or TiO under similar conditions [44]. The nucleation of brookite was related to the brookite-like structure stabilized by NaF.

These first reports indicate that the formation of pure brookite strongly depends on many factors, which are difficult to predict. For example, Mitsuhashi and Watanabe [45] synthesized brookite from fresh coprecipitates obtained by neutralization with NaOH of an aqueous solution of $TiCl_4$ and $CaCl_2$ at 220–560 °C for 0.5–220 h. Their conclusion was that also the $Ca^{2+}$ ions, with an ionic radium similar to that of the $Na^+$ ions, have a stabilization effect for the formation of brookite. Arnal *et al.* [46] observed the singular formation of brookite by the reaction of *tert*-butyl alcohol with $TiCl_4$ at 110 °C. The crystallization of brookite was related to the formation of a unique hydroxyl group during the alcoholysis of $TiCl_4$.

Brookite was hydrothermically synthesized at 110–200 °C within 24 h using amorphous $TiO_2$ and sodium salts as starting materials [47]. Almost single phase brookite was obtained at 200 °C and a $TiO_2$/NaOH molar ratio ~1. It was suggested that in alkaline solution the crystallization of brookite from sodium titanate occurred with release of $Na^+$ and $H^+$ ions accompanied by the oxidation of Ti and Ti-OH bond that changed to Ti-O-Ti bond in the structure.

To avoid any contamination with the other polymorphic $TiO_2$ phases, Kominami *et al.* [48] synthesized microcrystalline brookite by solvothermal treatment of oxobis(2,4-pentanedionato-O,O')titanium ($TiO(acac)_2$) in ethylene glycol, in the presence of sodium laurate and a small amount of water at 300 °C. As confirmed by Raman spectroscopy, pure brookite was obtained when Na/Ti = 2. Ethylene glycol showed a specific solvent effect for the crystallization of brookite.

Zheng *et al.* [49,50] synthesized brookite nanocystallites by using $Ti(SO_4)_2$ or $TiCl_4$ as the precursors. The formation of brookite was obtained under hydrothermal treatments by controlling the pH values and the reaction temperature. Different conditions were used depending on the titanium precursor. High basicity favoured the formation of brookite in the presence of $TiCl_4$ solutions.

In the last decade, an always increasing number of papers have concerned the preparation of powders and films of brookite. Inorganic and organic precursors such as $TiCl_4$ [21,24,49–58], $Ti(SO_4)_2$ [18,59–62], $TiOSO_4$ [63,64], $TiCl_3$ [3,19,65–68], $TiOCl_2$ [16,69,70], titanate nanotubes [69,71–73], titanium tetraisopropoxide [25,74–76], titanium butoxide [77–81] and titanium tetraethoxide [82] have been employed.

Pottier *et al.* [51] synthesized nanoparticles of brookite and rutile by thermolysis of $TiCl_4$ in concentrated HCl solutions at 100 °C. The Ti:Cl molar ratio was the key factor to determine the crystalline phases and their relative proportions. Pure brookite was easily separated by the mixtures of brookite and rutile by drying the stable brookite sols obtained by peptization of the solid phase with a $HNO_3$ solution [51] or by repeated washings with water [24]. Similarly, platelets of brookite were obtained by selective peptization of the mixtures of brookite and rutile resulting from the thermolysis of $TiCl_4$ (0.15 mol $L^{-1}$) in a $HNO_3$ solutions at 95 °C for 7 days [56]. Lee and Yang [55] synthesized crystalline $TiO_2$ nanoparticles with pure brookite structure by hydrolysis of $TiCl_4$ in $HNO_3$ solutions at 70 °C within 40 h. The aqueous $TiCl_4$ solutions contained not more than 0.8 mol $L^{-1}$ of $Ti^{4+}$ and the concentration of $HNO_3$ was kept in the range of about 3.9–4.3 mol $L^{-1}$. Nanocrystalline particles of pure brookite were prepared by an ambient condition sol process hydrolyzing $TiCl_4$ in an acidic alcohol solution under refluxing [53,54]. The refluxing time and temperature had a fundamental role in controlling the particle size and the phase of the particles obtained [54]. These results highlight the

strong influence of the precipitation conditions (acidity, nature of the anions, titanium concentration, *etc.*) on the formation of brookite.

Yang *et al.* [59] prepared pure brookite by using $Ti(SO_4)_2$ as the precursor. The phase formation was achieved by hydrothermal treatment at 200 °C for 24 h. $Ti(SO_4)_2$ was hydrolyzed using 2 M NaOH and a NaOH/ $Ti(SO_4)_2$ molar ratio of 4:1. Xie *et al.* [18] observed that the crystallinity of brookite increased with increasing the hydrolysis time. Ultrafine brookite powders were prepared by Luo *et al.* [62] by hydrolyzing $Ti(SO_4)_2$ in alkali at 199 °C under high pressure.

Pure brookite was synthesized by thermolysis of an aqueous solution of $TiOSO_4$ at 90 °C for 4 h [63,64]. In the presence of lithium oxalate with a molar ratio $[C_2O_4^{2-}]/[Ti^{4+}] = 1$, a titanium oxalate-based compound $Ti_2O_3(H_2O)_2(C_2O_4)\cdot 3H_2O$ formed. Brookite was obtained by thermal decomposition of the oxalate hydrate at a temperature as low as 300 °C [63]. Samples with high specific surface area lying between 150 and 400 $m^2\ g^{-1}$ were obtained by thermal decomposition of the oxalate hydrate at a temperature between 300 and 400 °C for 4 h under an air atmosphere [64]. As shown in Figure 7, the eggshell morphology of the $Ti_2O_3(H_2O)_2(C_2O_4)\cdot 3H_2O$ compound was retained despite the creation of porosities arising from the removal of water and oxalate species.

Many years after the first pioneering work of Kiyama *et al.* [41], a few reports have concerned the synthesis of brookite by thermolysis of $TiCl_3$ in aqueous media. Li *et al.* [65,83], prepared phase-pure brookite of high crystallinity under ambient pressure at 70°C via reacting a mixed solution of urea and titanium(III) chloride. The resultant particles were monodispersed spheres (~154 nm) composed of brookite nanocrystals (~25 nm) that were stable in terms of phase purity and morphology up to ~ 500 °C. Particles with lower size distribution were obtained by adding polyethylene glycol to the solution of $TiCl_3$ and urea [66]. Štengl *et al.* [67] prepared transparent particles of brookite by hydrolysis of an aqueous solution of $TiCl_3$ in the presence of a solution of polyethylene glycol in ethanol at 70 °C. Selected area electron diffraction (SAED) analysis showed that the brookite particles grew in the presence of polyethylene glycol with a molar mass higher than 10,000. The crystallinity of the samples increased with the time of ageing in the aqueous solutions up to 60 days. Recently, pure brookite was obtained by hydrothermal treatment of $TiCl_3$ with $NH_4OH$ at 200 °C for 20 h in the presence of 4.2 M NaCl [68].

The mechanism of the direct formation of titanium(IV) oxide from a titanium(III) solution is still unclear. Li *et al.* [3] selectively synthesized brookite nanocrystals via a redox route under mild hydrothermal conditions (180 °C, 3 h), employing $TiCl_3$ as the titanium source and $H_2O_2$ as the oxidant. Pure brookite was attained by carefully controlling the reactant concentration (0.0625–0.075 M) and the solution pH (1.1–1.32). Spindle-like particles of pure brookite were obtained at pH = 10 by using $NaNO_3$ as the oxidizing agent [19].

Small brookite particles were separated by centrifugation from a mixture of brookite and rutile obtained by self-hydrolysis of a solution of $TiOCl_2$ with HCl in autoclave for 24 h [69]. Liu *et al.* [70] synthesized nanocristalline brookite by thermohydrolysis of a titanium oxychloride hydrate obtained by slow hydrolysis of a commercial $TiOCl_2$ solution in a solution containing tetramethylammonium hydroxide (TMAOH) and $H_2O$. Brookite was obtained for $0.47 \leq Ti/TMAOH \leq 0.6$.

**Figure 7.** SEM images of: (**a**) $Ti_2O_3(H_2O)_2(C_2O_4)\cdot 3H_2O$; (**b**) brookite obtained by thermal decomposition at 300 °C [63].

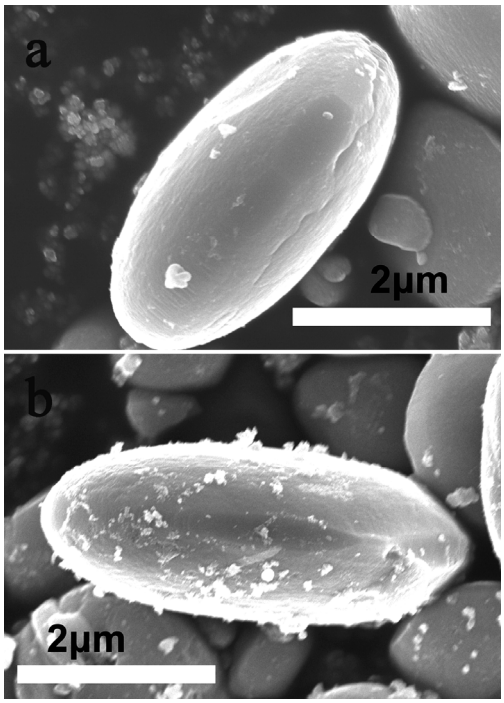


Nanocrystals with brookite phase were prepared by Murakami *et al.* [73] by hydrothermal treatment of the solution obtained by dispersion of a commercial powder of titanate nanotubes in $HClO_4$. Single-phase brookite was extracted from the suspension by centrifugal separation.

Pure brookite nanoparticles were synthesized by hydrothermal treatment of amorphous titania prepared by reaction of titanium(IV) isopropoxide with water in ethanol [74]. The amorphous titania was successively treated with NaOH and water at 200 °C for 48 h. Titanium isopropoxide vapour, argon and oxygen mixtures were used to obtain pure brookite crystals with large surface area by plasma enhanced chemical vapour deposition (PECVD) at room temperature, under an applied d.c. bias voltage of −250 V [75]. Complex porous particles of brookite were prepared using hydrated pollen grains exposed to titanium isopropoxide solutions, followed by calcination at 500 °C for 3h [76].

Recently, pure brookite has been successfully synthesized by hydrothermal treatment of water-soluble titanium complexes [84] such as titanium-peroxo-glycolate [16,85–88] and titanium bis(ammonium lactate) dihydroxide [23,89].

A selective synthesis of brookite was realized by Tomita *et al.* [85] by using an aqueous solution containing the titanium-peroxo-glycolate complex $(NH_4)_6[Ti_4(C_2H_2O_3)_4(C_2H_3O_3)_2(O_2)_4O_2]\cdot 4H_2O$ prepared from Ti powder dissolved in an ice-cooled solution of 30% $H_2O_2$, 28% $NH_3$ and glycolic acid. Single-phase brookite nanorods were obtained at 200 °C for 24 h, by adjusting the pH of the solution to 10 by addition of $NH_3$ or ethylenediamine [86]. The results demonstrated that a weakly basic environment was essential for the formation of brookite while ammonium ions did not play an important role. Pure brookite was also obtained by Štengl and Králová [16] by hydrothermal treatment of a solution of titanium peroxo-glycolate complex at pH 9.5 and 220 °C for 24 h. The formation of brookite was attributed to the structure of the complex anion that contains four titanium atoms

coordinated by glycolic acid and peroxo groups in a dimer-like structure that is connected to another dimer through bridging oxo groups. As shown in Figure 8, this structure closely resembles the architecture of brookite [84].

Similarly, brookite particles with typical nanorod shapes were synthesized at pH 10 by hydrothermal treatment at 200 °C for 24 h of the titanium picolinato complex obtained by adding picolinic acid rather than glycolic acid to the peroxo-titanic acid solution [90].

**Figure 8.** Similar structures of the titanium peroxoglycolate complex and brookite [84].

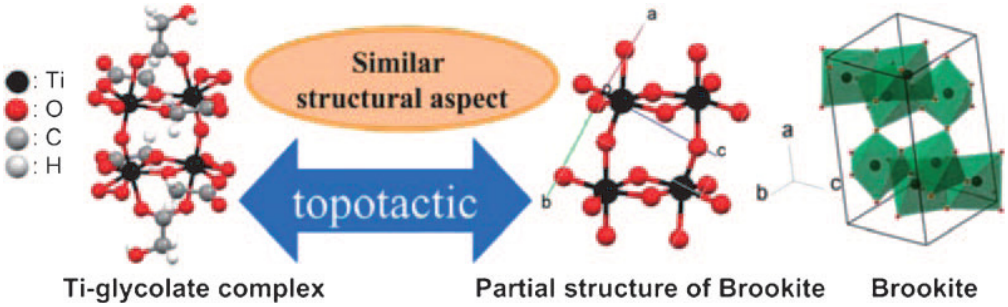


A microwave-assisted hydrothermal treatment of the titanium-peroxo-glycolate complex at 200 °C for 0–60 min allowed to synthesize brookite particles with a size smaller than that obtained by the conventional hydrothermal method [87]. Lately, nanocrystalline single phase brookite was also prepared by decomposition at 200 °C for 4 h of a water-soluble titanium complex with ethylenediaminetetraacetic acid (EDTA) [91]. When the titanium concentration in the starting solution was higher than 0.25 M, brookite could be prepared in a wide range of pH including both acidic and basic media.

Bahnemann *et al.* [23,89], synthesized brookite nanorods by a simple hydrothermal method at 160 °C for 24 h using aqueous solutions of commercially available titanium bis(ammonium lactate) dihydroxide (TALH) in the presence of urea as an *in situ* $OH^-$ source. High quality brookite was obtained at high concentrations of urea (≥ 6.0 M).

A drawback of the environmentally benign syntheses of single-phase brookite using water-soluble titanium compounds and water as solvent is the possibility to obtain anatase, rutile or mixed $TiO_2$ phases if the experimental conditions, e.g., water to precursor ratio, solution pH, reaction temperature, are not strictly controlled.

Brookite was also prepared from the lepidocrocite-type $K_{0.8}Ti_{1.73}Li_{0.27}O_4$ by alkali metal ion extraction with polytetrafluoroethylene (PTFE) and simultaneous heat treatment at 400 °C in flowing Ar [92]. Fully oxidized brookite formation and complete decomposition of the PTFE derivatives were achieved by further heating in flowing air, and coproduced alkali-metal salts were removed by washing with water.

Additionally, brookite was obtained by milling anatase-phase powders. Wakamatsu *et al.* [93] synthesized almost single phase brookite after 54 ks and 72 ks ball milling of anatase under the condition of medium intensity.

It is worth noting that the final products of several syntheses reported in the literature are not really single phase brookite since they contain traces of anatase or rutile, as clearly evidenced by the XRD patterns. Reyes-Coronado *et al.* [17] prepared brookite nanoparticles by hydrothermal treatment of amorphous titania obtained by titanium(IV) isopropoxide, water and 2-propanol. The white paste of

amorphous titania was diluted with 3 M HCl and heated at 175 °C for 7 h. Under these conditions the phase purity of brookite was over 95% due to the presence of a small amount of rutile.

Likewise, $TiO_2$ nanoparticles with brookite as the majority phase (> 95%) were synthesized by co-thermohydrolysis at 60 °C of an equimolar solution of $TiCl_3$ and $TiCl_4$ [94]. The pH was adjusted to 4.5 with a NaOH solution and the obtained suspension was aged for one week at 60 °C without stirring. The particles were flocculated by increasing the pH up to 6 with NaOH.

### *3.2. Brookite Nanomaterials*

Nanomaterials with special structures and morphologies, such as nanotubes, nanorods, nanospheres or nanoflowers have attracted growing interest because of their unique structures and properties. A summary of methods used to prepare brookite nanomaterials is reported in Table 1.

Nanometric particles of pure brookite $TiO_2$ were synthesized by modified thermolysis of reactant solutions containing titania powder, HCl, urea and PEG 10000 [66]. Unique flower-like brookite agglomerates with an average diameter of ~400–450 nm composed of single brookite nanocrystals of ~ 4–5 nm were obtained at 105 °C.

Deng *et al.* synthesized pure brookite nanotubes with a ~5 nm inner diameter and a ~0.78 nm interlayer space [71] or nanorods with a bipyramidal shape [72] using as precursors titanate nanotubes or nanosheets prepared by dispersing anatase $TiO_2$ powder in a 10 M NaOH solution at 120 °C or 90 °C, respectively. The corresponding brookite nanostructures were obtained by hydrothermal treatment at 200 °C.

Buonsanti *et al.* [57] developed a surfactant-assisted non aqueous strategy to prepare anisotropic brookite nanocrystals with tunable geometric features. The syntheses relayed on the high temperature aminolysis of titanium carboxylate complexes obtained by heating mixtures of $TiCl_4$, oleic acid and oleyl amine in 1-octadecene at 290 °C for 30 min under air-free conditions.

Well-facetted brookite crystals with the growth direction along the (001) axis were sinthesized by a low-temperature process using $[Ti_8O_{12}(H_2O)_{24}]Cl_8 \cdot HCl\ 7H_2O$ prepared by hydrolysis of a commercial $TiOCl_2$ solution and tetramethylammonium hydroxide with a molar ratio $R$ = Ti/TMAOH = 0.6 [70].

**Table 1.** Preparation of brookite nanomaterials.

| Morphology | Precursor | Synthesis route | Reference |
|---|---|---|---|
| nanocrystals | titania powder | hydrothermal treatment | [66] |
| nanotubes | titanate nanotubes | hydrothermal treatment | [71] |
| nanorods with bipyramidal shape | titanate nanosheets | hydrothermal treatment | [72] |
| nanorods | titanium oleate complex | high-temperature aminolysis | [57] |
| nanoplatelets | titanium oxychloride hydrate | solvothermal treatment | [70] |
| nanosheets | titanium lactate | hydrothermal treatment | [27] |
| nanoflowers | titanium oxysulfate | hydrothermal treatment | [5] |
| nanoflowers | titanium butoxide | hydrothermal treatment | [79] |

**Table 1.** *Cont.*

| | | | |
|---|---|---|---|
| humming-top-like nanostructures | titanium isopropoxide | hydrothermal treatment | [25] |
| macroporous spherical nanoparticles | brookite nanoparticles | spray drying with colloidal templating | [96] |
| hollow nanospheres | titanium-peroxo-glycolate complex | deposition on spherical polystyrene and hydrothermal treatment | [97] |
| pseudo-cube shaped nanocrystals | titanium-peroxo complex | oleate-modified hydrothermal treatment | [95] |

Lin *et al.* [27] synthesized brookite nanosheets with a regularly truncated tetragonal shape through a low-basicity hydrothermal process utilizing $TiCl_4$ as titanium source, urea as *in situ* $OH^-$ source, and sodium lactate as complexant and surfactant. After 12 h of reaction at 200 °C, the $[Ti(C_3H_4O_3)_3]^{2-}$ complex transformed into single-crystalline nanosheets with specific facets exposed.

High quality brookite flowers were obtained by Hu *et al.* [5] by hydrothermal treatment at 220 °C for 48 h of a suspension containing $TiOSO_4$ and NaOH at pH 12.5. Time-resolved experiments revealed that layered titanate transformed into spindle-like brookite nanoparticles that aggregated together to yield the flower morphology. The presence of $Na^+$ ions was a key factor for the formation of brookite since the replacement of NaOH with LiOH or KOH favoured the formation of mixtures of anatase and rutile.

Brookite nanoflowers consisting of single crystalline nanorods were prepared by hydrothermal treatment of a solution containing titanium butoxide, NaCl and aqueous ammonia [78–80]. Pure brookite was obtained with a NaCl concentration of about 0.25 M at 180 °C and 0.50–0.75 M at 200 °C [79]. At the initial stage of the reaction, layered titanate formed by condensation of $TiO_6$ octahedra. After several hours of heating, the layered structure collapsed resulting in the formation of brookite.

Nguyen-Phan *et al.* [25] prepared hierarchical brookite with a humming-top-like morphology by heating a solution containing 0.1 M NaOH, titanium isopropoxide and 2-propanol at 200 °C for 72 h. The gradual transformation from layered titanate to brookite phase was well consistent with the hypothesized formation mechanism of the hierarchical superstructure.

Macroporous spherical brookite particles with sub-micrometer diameters were prepared by spray drying and evaporation of an aqueous suspension obtained by mixing a commercial suspension of brookite nanoparticles and spherical monodispersed polystyrene latex particles, which were used for colloidal templating [96]. Katagiri *et al.* [97] prepared hollow brookite spheres by alternate deposition of titanium-peroxo-glycolate complex and a positively charged polyelectrolyte on spherical polystyrene templates, by utilizing the electrostatic interactions for the shell formation. The hollow capsules obtained by removing the polystyrene cores by tetrahydrofuran were hydrothermally treated at pH 10 and 200 °C for 24 h to induce the crystallization of brookite.

Pseudo-cube shaped brookite nanocrystals with the four corners truncated were synthesized by hydrothermal treatment of a solution of titanium-peroxo-glycolate complex in the presence of sodium oleate at 200 °C for 6 h [95]. The particular morphology of the particles (Figure 9) was attained by

selective absorption of oleate molecules onto specific crystal faces of brookite that reduced their specific surface energies and induced the formation of the cubic shape.

**Figure 9.** HRTEM image and diffraction pattern of a pseudo-cube shaped brookite particle [95].

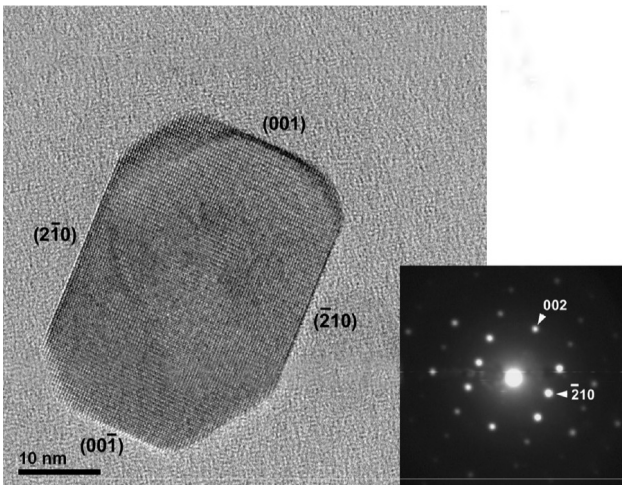


*3.3. Brookite Films*

Brookite is very difficult to prepare in thin-film form since most of the usually employed techniques lead to amorphous or crystalline anatase. Takahashi *et al.* [98] were the first to prepare almost pure brookite films by vapor phase decomposition of tert-butyl titanate. Evidence for the formation of a brookite layer as an intermediate of the anatase/rutile transition was also observed by *in situ* Raman spectroscopy after controlled oxidation of a Ti electrode in KOH electrolyte [99,100].

Moret *et al.* [101] prepared thin films of $TiO_2$ by pulsed laser deposition at 750 °C on silicon and other substrates. The laser-ablation target was a pellet prepared from a 99.95% $TiO_2$ powder. Brookite was the main phase present in the films, along with anatase and a small amount of rutile. Djaoued *et al.* [102] obtained brookite-rich films by using titanium tetraisopropoxide, diethanolamine and polyethylene glycol. The brookite phase was found preponderant only in films heated slowly to 600 °C. The weight fraction of brookite in the crystalline phase was around 70%.

Shibata *et al.* [28] deposited $TiO_2$ films on $SiO_2$-coated glass plates using a commercial brookite type sol, followed by calcination at 500 °C for 30 min. The films contained anatase and the content of brookite was about 75%. The same commercial sol was employed by Jiang *et al.* [103] to prepare mesoporous films that were tested as electrodes for dye-sensitized solar cells.

63.4% of brookite and 36.6% of anatase were present in a $TiO_2$ thin films deposited on a soda-glass substrate using a sol suspension obtained by hydrolysis of titanium tetraisopropoxide [104]. Only pure anatase was observed if the substrate was silicon. The formation of the brookite phase was attributed to the presence of Na dissolved from the soda-glass substrate during the calcination at 500 °C for 2 h.

Mild oxidation of Ti foils in air at 500 °C for 6 h resulted in brookite-rich films characterized by a strong absorption band in the visible spectral range [105].

Kuznetsova *et al.* [4] obtained pure brookite thin films by using $TiCl_4$, cellulose, ethylene glycol and oxalic acid as complexing agent. The XRD results revealed an unusual (121) orientation of the

film due probably to a suitable selection of the chemical processing parameters. The presence of 5% of $Na^+$ ions detected by XPS analysis confirms that the thermo-diffusion process of Na from the glass substrate induces the stabilization of brookite [106]. Single (121) oriented pure brookite films were also deposited on glass substrates using a solution of titanium butoxide and acetic acid [81]. The particle size was controlled by the water/acetic acid ratio.

Transparent $TiO_2$ thin films were deposited on soda lime glass at different substrate temperatures by a spray pyrolysis technique from an aqueous peroxo-polytitanic acid solution [107]. A low polycrystalline brookite structure was obtained when the amorphous as-deposited films were annealed in air at 500 °C for 3 h.

Novotna *et al.* [108,109] prepared pure brookite thin films by a very simple sol–gel method. Soda lime glasses were dipped into a solution of titanium isopropoxide, HCl, 2-propanol, and acetylacetone at 22 °C. Finally, the coated substrates were calcined at 500 °C for 2 h. The formation of the brookite phase was caused by the diffusion of sodium ions from the soda lime substrate.

An alternative possibility for the formation of brookite films is the synthesis of brookite particles and their following deposition on a substrate. Thin films were so obtained by coating stable sols of pure brookite separated from mixtures of brookite and rutile by peptization with $HNO_3$ [21,58], or by repeated washings with water [110–112]. Magne *et al.* [22,113] prepared pure brookite porous films using a viscous paste created by mixing ethyl cellulose powder dissolved in ethanol and brookite particles obtained from mixtures of brookite and rutile or by cohydrolysis of $TiCl_3$ and $TiCl_4$.

Kim *et al.* [114] prepared brookite colloidal sols for thin film coating by hydrothermal treatment at 120 °C for 10 h of the solution obtained dissolving Ti hydroxide in $H_2O_2$ in the presence of 5 M NaCl. Recently, nanostructured brookite films were deposited by the matrix-assisted pulsed laser evaporation technique [115,116]. The target was a frozen toluene suspension of brookite nanorods covered with an oleate/oleyl ammine capping layer synthesized by surfactant-assisted aminolysis of titanium oleate complexes at 280 °C under air-free conditions [57].

## 4. Photoactivity

### *4.1. Pure Brookite*

The difficulty in preparing brookite having both high purity and large surface area is probably one of the reasons for the limited works on its photocatalytic properties. Anyway, density functional theory calculations have shown that the commonly exposed brookite (210) surface is more reactive than the ubiquitous anatase (101) surface and might be useful in catalytic and photocatalytic applications [117].

The first study on the photocatalytic behaviour of brookite appeared many years after the publication of the pioneering works on the preparation of this $TiO_2$ polymorph [39–41,43–45]. In 1985, Ohtani *et al.* [42] found that extra-fine crystallites of brookite, prepared by air oxidation of $TiCl_3$ in aqueous HCl solution, possessed good photocatalytic capacities for both the reactions of $H_2$ formation from 2-propanol and $O_2$ evolution from an $Ag_2SO_4$ solution. In 2003, Kominami *et al.* [118,119] studied the correlation between physical properties and photocatalytic activities of nanocrystalline brookite samples prepared by a solvothermal method. The powders were calcined at various temperatures and then tested for the photocatalytic mineralization of $CH_3COOH$ in aqueous solutions

and dehydrogenation of 2-propanol. Some samples exhibited photoactivities comparable to that of the representative active commercial photocatalyst, Degussa P25.

Nanocrystalline brookite particles obtained by reaction of $TiCl_3$ and urea at 70 °C revealed a good efficiency for the photodegradation of acetaldehyde [65] and 4-chlorophenol [66] but the activity of these samples was rather lower than that of Degussa P25.

Brookite was found efficient for the degradation of rhodamine B [18] but less active than P25 [19]. Macroporous brookite particles prepared by a spray drying process with a precursor solution of brookite nanoparticles and polystyrene latex particles were more active for the degradation of rhodamine B than dense particles as a result of their increased surface area [96]. The macroporous particles retained their structure in the liquid phase and were easily collected and reused.

Kobayashi *et al.* [88] prepared brookite nanoparticles by hydrothermal treatment of a titanate-glycolate complex. The samples were more efficient than Degussa P25 for the photooxidation of NO. Under illumination by only visible light with $\lambda > 510$ nm the photoactivity was four times higher than that of P25 due probably to the presence of doping nitrogen atoms. The photocatalytic activity of samples annealed at different temperatures was examined by using the degradation of Orange II dye [16]. With increasing temperature, the crystallinity increased and the photoactivity was higher. An enhancement of activity was achieved by employing brookite particles with a smaller size obtained by microwave heating of the titanate-glycolate complex [87]. Further studies evidenced that brookite synthesized from a water soluble Ti-EDTA complex had a considerably higher activity for the decomposition of NO than that of brookite prepared from the titanate-glycolate complex [91].

Transparent particles of brookite prepared by hydrolysis of an aqueous solution of $TiCl_3$ in the presence of polyethyleneglycol degraded Orange II more efficiently than P25 [67]. Li *et al.* [3] selectively synthesized anatase, rutile and brookite nanocrystals via a redox route under mild hydrothermal conditions employing $TiCl_3$ as titanium source. The brookite nanoplates gave the best performance for the bleaching of methyl orange under UV irradiation.

Brookite nanoparticles prepared by hydrothermal treatment of a solution containing tetrabutyl titanate and triethanolamine at pH 12 were more active than anatase nanorods prepared at pH 11 and P25 [77]. The higher activity was attributed to the larger surface of the brookite nanoparticles.

Di Paola *et al.* [24] synthesized mixtures of brookite and rutile by thermohydrolysis of $TiCl_4$ in HCl solutions. The brookite particles separated by selective peptization revealed good catalytic properties for the photodegradation of 4-nitrophenol. The powder calcined at 450 °C exhibited a higher reactivity, mainly because of its increased crystallinity.

Similarly, the photocatalytic activity of small brookite nanoparticles separated by centrifugation from a mixture of brookite and rutile prepared by self-hydrolysis of $TiOCl_2$ at 100 °C was enhanced by a further hydrothermal treatment at 100 or 200 °C for 24 h [69].

Pure brookite nanorods synthesized by thermal hydrolysis of titanium bis(ammonium lactate) dihydroxide were less active than anatase for the reaction of photodegradation of dichloroacetic acid due probably to its lower surface area [23,89]. At variance, brookite was more efficient than anatase and P25 for the production of $H_2$ from an aqueous methanol solution. This behaviour was attributed to the position of the flatband potential of brookite that is more cathodic than that of anatase so that it has a higher driving force for the proton reduction.

Nanomorphologies generally show better photocatalytic properties because of their larger specific areas that provide more active sites. Brookite nanocrystals prepared by hydrothermal treatment of titanate nanotubes exhibited photocatalytic activity for the degradation of acetaldehyde similar to that of P25 [73]. Lin *et al.* [27] prepared high-quality brookite nanosheets surrounded with four (210), two (101), and two (201) facets. The photoactivity of these nanosheets for the degradation of methyl orange was superior to that of P25 in terms of unit specific surface area. Other morphologies such as irregularly faceted nanoflowers and nanospindles were inactive indicating that the photocatalytic activity of brookite is highly morphology-dependent.

Brookite nanoflowers degraded methyl orange much more efficiently than anatase nanorods with similar specific area [78]. The photocatalytic activity of the nanoflowers was high also for the degradation of phenol and salicylic acid [79].

Zhang *et al.* [82] modified the surface morphology of brookite nanorods by chemical etching with a solution containing $NH_3$ and $H_2O_2$ or with concentrated $H_2SO_4$. Before etching, the nanorods were more active than P25 for the decomposition of toluene. After etching with the $NH_3$-$H_2O_2$ solution the photocatalytic activity of the samples increased, whereas the treatment with $H_2SO_4$ caused an appreciable reduction of activity. The enhancement of photoactivity was ascribed to the formation of highly active faces working as oxidation sites.

Addamo *et al.* [110] prepared thin brookite films that exhibited a high photocatalytic activity for 2-propanol and a promising long term stability after repeated usage. Low crystallized brookite films deposited by spray pyrolysis from a peroxo-polytitanic acid were active for the photodegradation of methylene blue [106].

Mattson and Österlund [20] presented a comparative study of the adsorption and photoinduced degradation of propanone and acetic acid on thin films of anatase, brookite, and rutile. The quantum yield for the photodegradation of propanone was larger for brookite than for anatase and much larger than for rutile. In contrast, the quantum yield for the degradation of acetate was lower for brookite than for anatase.

Anatase films deposited on soda lime glass precoated with a $SiO_2$ layer exhibited better activity for the photodecomposition of acid orange 7 and 4-chlorophenol than brookite films obtained on soda lime glass [108]. Similar results were reported by Krýsa *et al.* [109]. The low photocatalytic activity was attributed not to the presence of brookite but to the high content of $Na^+$ ions diffused in the film from the glass substrate.

Anatase and brookite-rich films tested for the photocatalytic oxidation of methylene blue and *cis*-9-octadecenoic acid exhibited almost the same activity [28]. Anyway, the brookite-rich film was more hydrophilic than the anatase film as revealed by the lower contact angle under weak UV light irradiation. Zhou *et al.* [120] prepared anatase/brookite films on modified poly(ethylene terephthalate) substrates that were less active than anatase films for the photodegradation of rhodamine B but showed an improved hydrophilicity when brookite was present in the films.

Superhydrophilic properties, even in dark conditions, were exhibited by transparent brookite thin films prepared by using titanium tetraisopropoxide as the precursor [108]. Similar results were obtained by Bellardita *et al.* [121] who studied the photocatalytic activity and the hydrophilicity of anatase, brookite and rutile films deposited by sols obtained by thermolysis of $TiCl_4$ in aqueous or

diluted HCl solutions. As shown in Figure 10, the anatase and rutile films were less hydrophilic than the brookite film that exhibited a contact angle of 10° in the dark.

**Figure 10.** Contact angles exhibited by films of rutile, anatase and brookite.

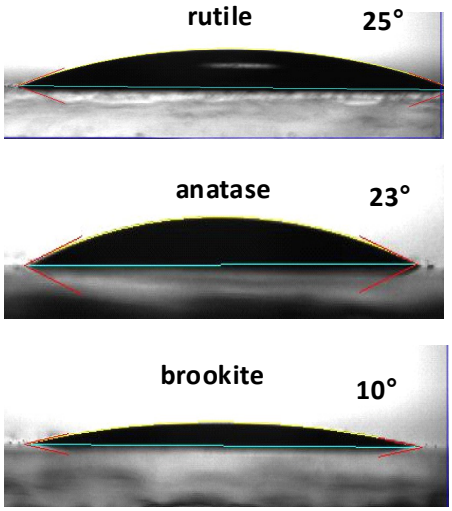


In addition, N-doped brookite films showed a photoinduced hydrophilic ability highest than that of N-doped anatase and rutile films [122].

Brookite has been successfully tested for the photocatalytic production of hydrogen. Ohtani *et al.* [42] firstly reported that pure brookite powder, modified by Pt nanoparticles deposition, had a marked photocatalytic activity for the dehydrogenation of 2-propanol. A brookite sample with improved crystallinity and sufficient surface area obtained by calcination at 873 K exhibited the hydrogen evolution rate almost equal to that of P25 [118,119]. Chiarello *et al.* [123] proved that Pt-deposited brookite is a very good photocatalyst for obtaining hydrogen from methanol steam reforming under UV-vis irradiation, also in consideration of its high selectivity to $CO_2$ formation and low CO production. Kandiel *et al.* [23] reported that the photocatalytic hydrogen evolution of anatase/brookite mixtures and pure brookite was higher than that of pure anatase. Anatase-brookite-rutile mixtures with brookite as the major phase were superior to P25 and anatase in generating hydrogen from an aqueous EDTA solution under visible light [124].

Anji Reddy *et al.* [125] demonstrated the facile insertion of lithium into nanocrystalline brookite due to the presence of atom-free channels along the (001) direction that enable the lithium mobility into the structure (see Figure 2). Electrochemical and ex situ XRD studies showed that brookite is stable for lithium intercalation and deintercalation. The high reversible capacity and low polarization make brookite an attractive alternative negative electrode material for Li-ion batteries. Further studies revealed that the reversibility of Li insertion decreased with an increase in crystallite size of brookite [126]. Hybrid multi-walled carbon nanotube/brookite electrodes improved the specific capacity and capacity retention on cycling [127,128]. Dambournet *et al.* [63] prepared micrometer-size mesoporous brookite electrodes with a high specific area that provided higher volumetric energy density in a lithium ion battery than anatase or rutile electrodes.

Brookite-rich thin films obtained by oxidation of Ti foils in air in a temperature range from 500 to 700 °C were tested as electrodes for water splitting, under visible light [129]. The photocurrent

densities were higher than those observed with anatase or rutile produced by oxidation of Ti foils. Mesoporous brookite films containing a certain amount of anatase were used as electrodes for dye-sensitized solar cells [103]. Magne *et al.* [22] prepared efficient cells employing porous layers of pure brookite. The comparison between anatase and brookite based-cell revealed that the latter phase is very interesting for this kind of applications [22].

Photocatalysis by $TiO_2$ has been mainly applied to degrade organic and inorganic pollutants both in vapor and in liquid phases. Until a few years ago, the photocatalytic reaction processes were considered highly unselective, particularly in water, but recent researches have demonstrated that it is possible to perform organic selective reactions for synthetic purposes. Very few examples of such reactions in aqueous solutions have been reported [129,130].

Brookite was also tested for the selective oxidation of 4-methoxybenzyl alcohol to 4-methoxybenzaldehyde (*p*-anisaldehyde) in water [131–133]. A good conversion and selectivity (52.5%) was obtained after reasonable irradiation times. The selectivity of the brookite sample was more than 3 and 6 times higher than that obtained with a commercial anatase or P25, respectively. The highest oxidizing rate of the commercial samples corresponded to a lower selectivity for the partial oxidation of the aromatic alcohol.

Defective brookite obtained by helium pretreatment of brookite prepared by thermal hydrolysis of titanium bis(ammonium lactate) dihydroxide was more active than the untreated sample for the photocatalytic reduction of $CO_2$ [134]. The production of CO and $CH_4$ was remarkably higher than that observed with defective and defect-free anatase and rutile. The enhancement was attributed to a facilitated formation of oxygen vacancies on brookite that could promote $CO_2$ activation both in the dark and under illumination.

### *4.2. Doped and Loaded Brookite*

The band gaps of anatase, brookite and rutile allow only the absorption of the ultraviolet part of the solar irradiation so that many researches have recently been carried out to obtain materials doped with either anions or cations or co-doped with several ions to shift the absorption edge to longer wavelengths. N-doping was found to be particularly effective in enhancing the photocatalytic efficiencies of $TiO_2$ in the visible-light range [135].

Yin *et al.* [122,136–138] prepared N-doped brookite nanoparticles by a solvothermal treatment at 190 °C of aqueous or alcoholic solutions of $TiCl_3$ and hexamethylenetetramine. The samples showed higher photocatalytic activity than that of P25 for the oxidative destruction of nitrogen monoxide under irradiation with visible light ($\lambda > 510$ nm) and UV-light ($\lambda > 290$ nm).

Au-loaded brookite samples prepared by photodeposition from a $HAuCl_4 \cdot 4H_2O$ solution were more active than pure brookite for the degradation of rhodamine B under visible light irradiation [139]. It is worth noting that highly stable catalytic systems for CO oxidation were obtained by depositing gold on the surface of brookite [140]. The interaction between gold nanoparticles and brookite plays the important role of stabilizing the catalyst against sintering in high temperature environments.

Lanthanide-doped $TiO_2$ samples have received an increasing attention for their enhanced photocatalytic properties. The increase in activity was attributed to a higher adsorption of the organic pollutants due to the formation of Lewis acid-base complexes between the f-orbitals of the lanthanides

and the substrates [141,142]. Bellardita *et al.* [121,143], firstly, synthesized Sm-loaded brookite powders and films that were tested for the photodegradation of 4-nitrophenol and 2-propanol, respectively. Loading with Sm resulted in a significant improvement of the photoreactivity of brookite and the beneficial effect was ascribed to an increased separation efficiency of the photogenerated electron–hole pairs. Lanthanum-doping was also positive to improve the photocatalytic efficiency of brookite [94] and lanthanum-doped brookite films were studied for dye-sensitized solar cells [113].

The surface hydrophilicity of $TiO_2$ thin films can be increased by doping [144]. Eshaghi and Eshaghi [145] studied the effect of Cu loading on the surface properties of brookite thin films. The results indicated that the Cu-loaded brookite film was more hydrophilic than the undoped film both under irradiation and in the dark.

The addition of samarium to anatase, brookite and rutile films caused a reduction of the contact angle values [121]. In particular, the Sm-loaded brookite film revealed a nearly superhydrophilic property exhibiting a 3° water contact angle in the dark. The enhanced hydrophilicity was attributed to an increased surface hydroxyl concentration due to the presence of the rare earth metal f orbitals.

Molybdenum/carbon co-doped brookite samples prepared by hydrothermal treatment of $Ti(SO_4)_2$ in the presence of glucose and ammonium molybdate were active for the photodecoloration of rhodamine B under simulated solar light irradiation [146].

### *4.3. Mixtures of Brookite with Anatase and/or Rutile*

A not adequate attention has been paid to the photocatalytic activity of binary and ternary mixtures of brookite with anatase and rutile. Really, the photocatalytic activity of mixed $TiO_2$ phases is often higher than that exhibited by the pure single polymorphs. Usually, the contemporaneous presence of different phases of the same semiconductor is beneficial to enhance the photoactivity and in particular, the very efficient commercial $TiO_2$ Degussa P25 is composed of anatase and rutile. As already demonstrated for other systems [147–149], the coupling of different semiconductors allows the vectorial displacement of electrons from one semiconductor to another, leading to more efficient electron/hole separation and greater catalytic reactivity (see Figure 11).

Anyway, Ovenstone [150] observed that biphasic particles containing both anatase and brookite had lower photocatalytic activity than anatase for the decomposition of acetic acid. Similar behaviour was also found for anatase-brookite crystals that were tested for the gas phase oxidation of benzene [151,152]. It is worth noting that the amount of brookite present in these samples was very small.

Yu *et al.* [153–156] reported that anatase-brookite composite nanocrystals synthesized by a sonochemical sol-gel method were more active than anatase [153,154] and P25 [153,155,156] for the oxidation of propanone in air. Ozawa *et al.* [157] found that the photoactivity of an anatase-brookite sample for the oxidation of gaseous $CH_3CHO$ was 5.4 times greater than that of a single-phase anatase sample with comparable crystallite size and surface area. The high efficiency was attributed to the junction between anatase and brookite.

Anatase-brookite composites were more efficient than P25 for the photodegradation of methyl orange [78,79], methylene blue [158], rhodamine B [159–162], phenol [79,159], salicylic acid [79], acetaldehyde [163] and propanone in air [164,165].

The photoactivity exhibited by a mixture of anatase and brookite prepared from a titanium-lactate complex was slightly higher than that of pure brookite obtained from a titanium-glycolate complex [88]. Both samples were more active than P25 for the oxidation of NO whereas the anatase-brookite composite prepared from a peroxotitanium complex was less active than anatase for the degradation of methylene blue [166].

**Figure 11.** Schematic illustration of the electron/hole separation between two different semiconductors.

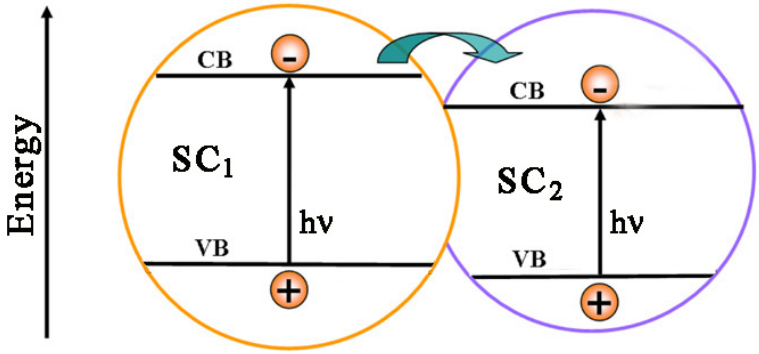


Qin *et al.* [167] synthesized nanosized $TiO_2$ particles using different alcohols as solvents, $TiCl_3$ and variable amounts of hexamethylene tetramine. Mixed crystals of anatase and brookite photodegraded methyl orange more efficiently than mixtures of anatase and rutile or pure anatase.

Ardizzone *et al.* [168] prepared anatase-brookite nanocrystals that showed an enhanced activity both for the degradation of $NO_x$ in gas phase and the oxidation of 2-chlorophenol in liquid phase. The photoactivity of the anatase–brookite composites was comparable to that of P25 [169] for the photoreduction of Cr(VI) but much higher for the degradation of toluene in gas phase [170].

Mesoporous anatase-brookite powders showed a high photocatalytic activity for the degradation of rhodamine B that was attributed to the porous structure, large specific surface area, bicrystallinity and small crystalline size [171]. A high photodegradation rate of rhodamine B was also exhibited by hollow submicrospheres with a rough surface synthesized via the combination of hydrothermal treatment and calcination of submicrospheres consisting of a polystyrene core and an amorphous $TiO_2$ shell [172].

Mahdjoub *et al.* [173] prepared anatase-brookite powders rich in brookite by hydrolysis of titanium tetraisopropoxide at room temperature. All the mixtures showed high photoactivity for the photodegradation of methyl orange and the best value was observed for the sample that contained the highest percentage of brookite.

The efficiency of the mixed samples depends on the percentages of the single $TiO_2$ polymorphs so that a great challenge is the possibility to tailor the composition of the biphasial mixtures. Mixed $TiO_2$ powders with brookite as the predominant phase were obtained in ambient conditions by hydrolysis of $TiCl_4$ in an acidic water-isopropanol medium [54,174]. The phase composition was tuned by varying the water-isopropanol ratio. The samples were active for the degradation of methyl orange under UV irradiation and a following treatment with *N*-methylpyrrolidone enhanced the photocatalytic activity under visible light [123,175–177].

Bahnemann *et al.* [23,89] synthesized anatase-brookite mixtures by thermal hydrolysis of a solution of titanium bis(ammonium lactate) dihydroxide in the presence of urea. The ratios between anatase and brookite were easily controlled by the concentration of urea. The anatase-brookite mixtures exhibited higher photocatalytic activity than anatase nanoparticles and P25 for the photocatalytic $H_2$ evolution from an aqueous methanol solution. On the contrary, the binary mixtures were less active than anatase for the degradation of dichloroacetic acid. For both reactions, the best sample contained 72% anatase and 28% brookite [89].

Shen *et al.* [68] synthesized $TiO_2$ polymorphs with a tunable anatase/brookite ratio by an alkalescent hydrothermal treatment of $TiCl_3$ in the presence of NaCl. The amounts of anatase and brookite were regulated by adjusting the NaCl concentration and the $NH_4OH/H_2O$ volume ratio. The photocatalytic activity of the mixed phases was higher than that of pure anatase and pure brookite for the degradation of rhodamine B and the best sample contained 46.6% anatase and 53.4% brookite. $TiO_2$ nanoparticles with controllable phases of anatase and brookite were also prepared by heating at 200 °C the suspension obtained by adding tartaric acid and NaOH to an aqueous solution of $TiCl_3$ and $NaNO_3$ [19]. The contents of anatase and brookite were tuned by varying the additional molar ratio of $C_4H_6O_6$ to Ti. The sample containing 78.7% anatase and 21.3% brookite exhibited the highest photocatalytic rate per surface area superior to that of brookite, anatase and P25.

Boppella *et al.* [162] prepared brookite/anatase and brookite/rutile nanocrystals by thermal hydrolysis of $TiCl_4$ in a water/ethanol solution. The tuning of the phase compositions was achieved by changing the water/ethanol ratio. Binary mixtures were more active than P25 and pure anatase for the degradation of rhodamine B under visible light.

Recent reports have confirmed the enhanced photocatalytic activity of binary mixtures containing brookite. Jiao *et al.* [80] prepared a series of anatase-loaded brookite nanoflower hybrids by hydrothermal treatment of a suspension of flower-like brookite, $NH_3 \cdot H_2O$ and tetrabutyl titanate. The powder containing 60% of brookite and 40% of anatase showed photoactivity superior to that of anatase and brookite for the degradation of methyl orange and 2,4-dichlorophenol.

Truong *et al.* [32] synthesized anatase-brookite composites from a titanium oxalate complex. The mixed samples were efficient for the reduction of $CO_2$ to $CH_3OH$ under both UV–vis and visible light irradiation, mainly due to the presence of doped carbon and nitrogen.

Anatase-brookite mesoporous nanoparticles showed a removal efficiency of Reactive Red 195 similar to that of commercial P25 under optimal conditions [178]. The percentages of anatase (76.8%) and brookite (23.2%) were very similar to the percentages of anatase and rutile in P25.

Nguyen-Phan *et al.* [25] synthesized a hierarchical rose bridal bouquet nanostructure containing a mixture of layered titanate and brookite that revealed an excellent performance for the degradation of methylene blue. The contemporaneous presence of two phases with different band gap energy facilitated the interfacial electron transfer, reducing the electron/hole recombination and promoting the degradation efficiency (see Figure 12).

Binary and ternary mixed $TiO_2$ phases supported on kaolinite were synthesized by introducing polymeric Ti cations into the layered aluminosilicate by hydrolysis of $TiCl_4$ in HCl [179]. The as-prepared samples exhibited strong photocatalytic activity for the removal of acid red G and 4-nitrophenol due to the synergetic effects of the adsorbibility of kaolinite and the catalytic ability of $TiO_2$. The best results were obtained with the anatase-brookite mixture.

The photocatalytic activity of the anatase-brookite composites depends on the relative percentages of the two phases (see Figure 13). A small or a large amount of brookite is generally unfavourable to improve the activity exhibited by pure anatase or brookite. As general trend, the photoactivity increases with increasing the amount of brookite, reaches a maximum and then decreases [68,80,89,162].

**Figure 12.** (**a**) Diffusion behavior of the charge carriers in layered nanosheets and (**b**) transport pathway of the excited electron in the mixed phase photocatalyst [25].

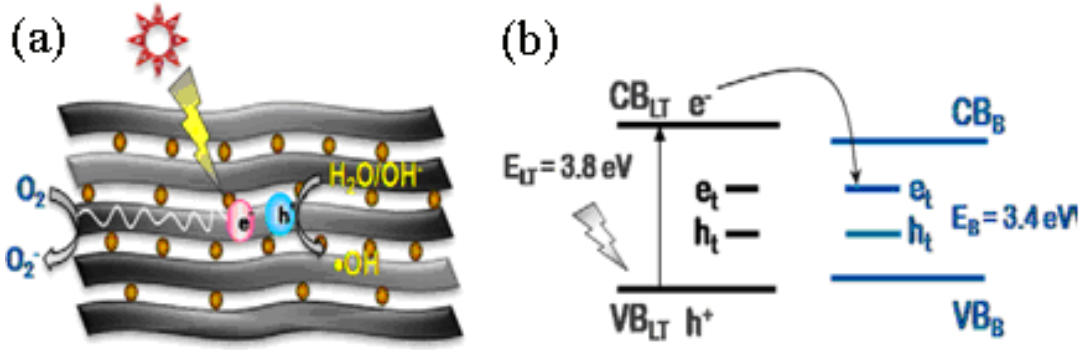


**Figure 13.** Photocatalytic degradation of methylene blue with various anatase-brookite mixtures and pure $TiO_2$ under UV irradiation [80].

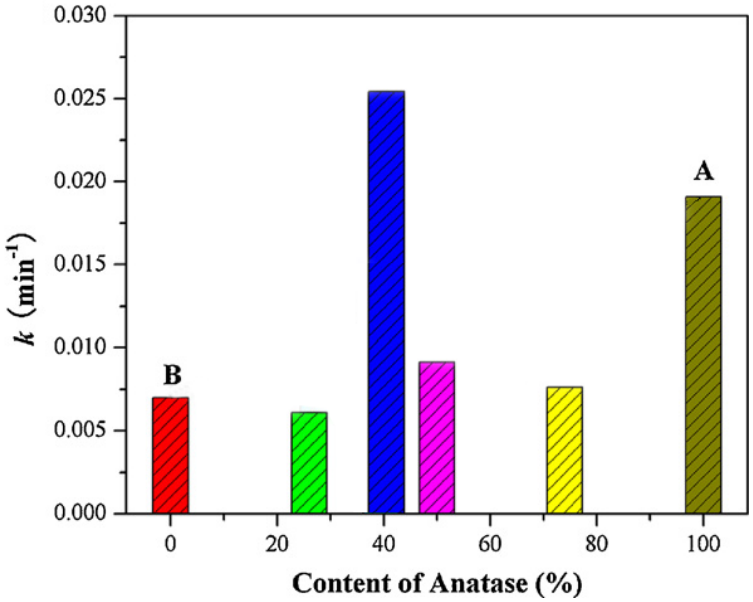


Several authors have reported an optimum ratio between anatase and brookite corresponding to the highest photoactivity for a given reaction. These ratios are often very different and depend on the particular method of synthesis. Besides, the range of examined compositions is often small. Only a few works have recently studied the behaviour of mixtures with brookite percentages ranging from 9.5 to 95% [23,68,89]. A rough comparison among the results of the previous investigations seems to suggest that the effective optimum amount of brookite ranges between 20 and 40%. Anyway, the behaviour of the various anatase-brookite composites also depends on many other factors such as specific surface area, crystallinity degree, crystallite sizes of the different phases, surface hydroxylation and preparation method, that can exert contemporaneously their influence on the photocatalytic process [180,181].

Only few papers have concerned the photocatalytic behaviour of brookite-rutile mixtures. Mixed brookite and rutile particles obtained by hydrothermal post-treatment of H-titanate fibers in an acidic solution were active for the degradation of rhodamine B [182]. Xu *et al.* [183] synthesized mixed brookite-rutile nanocrystals using $TiCl_4$ as titanium source and triethylamine as the "adjusting reagent" to tune the brookite/rutile ratio. All the binary mixtures degraded rhodamine B under artificial solar light and the photoactivity of the sample containing 38% brookite and 62% rutile was 6 times higher than that of P25. Similarly, a mixed sample with 83% brookite and 17% rutile prepared by thermal hydrolysis of $TiCl_4$ exhibited a photoactivity superior to that of P25 and pure anatase for the degradation of rhodamine B under visible light [162]. The improved performance of the brookite-rutile mixtures was attributed to the increased charge separation efficiency resulting from the interfacial electron transfer from brookite to rutile.

The performances of ternary mixtures of anatase, brookite and rutile have been also considered. Lopez *et al.* [184] firstly reported that an anatase-brookite-rutile mixture was more efficient than a mixture of anatase and brookite, anatase and P25 for the decomposition of 2,4-dinitroaniline. The highest activity was attributed to the lowest $E_g$ of the sample and to the coexistence of three different crystalline phases.

Anatase-brookite-rutile composites were active for the degradation of methyl orange [173], methylene blue [185], acetaldehyde [163], 4-nitrophenol [24] and 4-chlorophenol [66,183]. Samples with a mixed crystal lattice of anatase, brookite and rutile prepared by hydrolysis of titanium butoxide degraded $NO_x$ under UV and visible light illumination [186].

Ternary mixtures of the three $TiO_2$ polymorphs were obtained by thermolysis of solutions containing Ti powder, HCl, urea and polyethyleneglycol [66]. The photoactivity of the best sample, containing 3.2% brookite, 42.9% anatase and 53.9% rutile, was higher than that of brookite but lower than that of P25.

Di Paola *et al.* [30] synthesized highly active $TiO_2$ photocatalysts by thermohydrolysis of $TiCl_4$ in water at 100 °C. Binary mixtures of anatase and brookite and ternary mixtures of anatase, brookite and rutile were obtained depending on the $TiCl_4/H_2O$ ratio. The photoactivity of some samples was higher than that of Degussa P25 for the degradation of 4-nitrophenol. The most efficient sample contained 28% brookite, 65% anatase and 7% rutile.

Luís *et al.* [187] synthesized $TiO_2$ powders with different contents of anatase, brookite and rutile by hydrolysis of titanium tetraethoxide and post thermal treatment. The best results for the degradation of methylene blue were obtained with a binary mixture of anatase and brookite and a ternary mixture of the three $TiO_2$ polymorphs.

Recently, Liao *et al.* [188] synthesized anatase, brookite and rutile nanocomposites using toluene as the nonpolar solvent and toluene soluble tetrabutyltitanate as the precursor. The composition was easily tailored by varying the reagents volume ratio. The ternary mixtures were more efficient than P25 for the degradation of methyl orange. The photoactivity of the best sample, containing 29.9% anatase, 27.9% brookite and 42.2% rutile was almost twice as high as that of P25.

### *4.4. Doped and Loaded Mixtures of Brookite with Anatase and/or Rutile*

N-doped mixtures of brookite and rutile obtained by using 1-propanol or 1-butanol as solvents were less active than N-doped brookite [137]. Instead, N-doped (anatase-brookite) samples obtained in methanol were more active than N-doped anatase or N-doped (anatase-rutile) mixtures for the degradation of methyl orange under visible light [189].

Shao *et al.* [190] synthesized meso-macroporous N-doped $TiO_2$ materials with a bicrystalline (anatase and brookite) framework by thermal treatment of a mixture of hierarchical mesoporous-macroporous $TiO_2$ powder with an urea solution, followed by calcination at 350–550 °C. The samples showed a good photocatalytic activity for the photodegradation of methyl orange and rhodamine B under UV and visible-light irradiation. The photoactivity was significantly improved with increasing the nitrogen doping concentration.

Li and Liu [191] prepared N-doped (anatase-brookite) nanocatalysts by solvothermal treatment of titanium butoxide with dimethylformamide in the presence of acetylacetone at 180 °C. The binary mixtures were efficient for the degradation of methylene blue under both visible and UV light and the photoactivity of the most active sample containing 24.6% brookite and 75.4% anatase was comparable to that of P25. Visible light N-doped anatase-brookite mixtures were also obtained by hydrolysis of $TiCl_4$ in $CH_3COOH/HNO_3$ media followed by rapid calcination [192]. The samples were more active than a commercial N-doped anatase for the photodegradation of phenol and the visible light activity increased with increasing the brookite particle size.

$Fe^{3+}$-doped $TiO_2$ aerogels containing both anatase and brookite were more efficient than P25 for the salicylic acid degradation uder UV irradiation [193]. Hao and Zhang [194] prepared $Fe^{3+}$ and nitrogen co-doped mesoporous anatase-brookite mixtures by a modified sol-gel method from titanium butoxide using dodecylamine and $Fe(NO_3)\cdot 9H_2O$ as nitrogen and Fe dopants, respectively. The photoactivity of the co-doped powders for the degradation of 2,4-dichlorophenol under visible light irradiation was higher than that of the N-doped sample and P25.

Yu *et al.* [195] synthesized $F^-$-doped (anatase-brookite) powders by hydrolysis of titanium tetraisopropoxide in an $NH_4F$ aqueous solution. The photocatalytic activity of the $F^-$-doped samples for the oxidation of propanone under UV irradiation exceeded that of P25 when the $NH_4F/H_2O$ molar ratio was in the 0.5–3 range.

I-doped mixtures of anatase and brookite tested for the photocatalytic reduction of $CO_2$ in the presence of $H_2O$ vapor exhibited a significant enhancement of activity under both visible and UV–vis illumination [196].

Ag-loaded (anatase/brookite) powders synthesized via an alkalescent hydrothermal process were more efficient than the Ag-free composite and P25 for the degradation of methyl orange [197]. Yu *et al.* [198] prepared Ag–$TiO_2$ multiphase thin films on quartz substrates by liquid phase deposition from an aqueous solution of $(NH_4)_2TiF_6$, $AgNO_3$ and $H_3BO_3$, followed by calcination at 500 °C. The photocatalytic activity of the films consisting of anatase, brookite, rutile and silver nanoparticles exceeded that of an anatase film. High activity for the photodegradation of gaseous toluene was also exhibited by Ag–$TiO_2$ three-phasic powders synthesized from titanium butoxide and $AgNO_3$ using a microwave-assisted method [199]. The enhanced efficiency of the Ag–$TiO_2$ multiphase samples was attributed to the presence of many heterojunctions among the different $TiO_2$ phases and Ag.

Nassoko *et al.* [200] prepared Nd-doped (anatase-brookite) powders that showed better activity than the undoped $TiO_2$ mixture and P25 for the photodegradation of rhodamine B under visible light.

## 5. Conclusions

This review summarizes most of the papers concerning the synthesis and the photocatalytic characterization of brookite and brookite-based materials. Examples and details of the preparative methods as well as selected applications have been provided. Obtaining brookite is not as difficult as was believed until recently, but particular attention must be paid to avoid contaminations with other $TiO_2$ phases. Basic solutions are often necessary to obtain pure brookite but an accurate pH control is indispensable since lower pH values of the initial solution usually favour the formation of anatase. A reliable route is the easy separation of single phase brookite by peptization of dispersions of rutile-brookite mixtures obtained by thermohydrolysis of $TiCl_4$ in acidic solutions. Interesting "green chemistry" syntheses utilized water-soluble titanium complexes and water as the solvent.

Although some papers reported that brookite has sometimes higher photocatalytic activity than anatase and rutile, the use of pure brookite is not justifiable in heterogeneous photocatalysis either for photodegradation or photosyntetic reactions, due to the more laborious preparation methods. At variance, mixtures of brookite with anatase and rutile or with both anatase and rutile appear to be highly photoactive, particularly for photoxidation reactions both in solid-liquid and gas-solid systems, because of the presence of junctions among different polymorphic $TiO_2$ phases that enhance the separation of the photogenerated electron-hole pairs, hindering their recombination.

## References

1. Pauling, L.; Sturdivant, J.H. The crystal structure of brookite. *Z. Kristall*. **1928**, *68*, 239–256.
2. Bokhimi, X.; Morales, A.; Aguilar, M.; Toledo-Antonio, J.A.; Pedraza, F. Local order in titania polymorphs. *Int. J. Hydrogen Energy* **2001**, *26*, 1279–1287.
3. Li, J.-G.; Ishigaki, T.; Sun, X. Anatase, brookite, and rutile nanocrystals via redox reactions conditions: phase-selective synthesis and physicochemical properties. *J. Phys. Chem. C* **2007**, *111*, 4969–4976.
4. Kuznetsova, I.N.; Blaskov, V.; Stambolova, I.; Znaidi, L.; Kanaev, A. $TiO_2$ pure phase brookite with preferred orientation, synthesized as a spin-coated film. *Mater. Lett*. **2005**, *59*, 3820–3823.
5. Hu, W.; Li, L.; Li, G.; Tang, C.; Sun, L. High-quality brookite $TiO_2$ flowers: Synthesis, characterization, and dielectric performance. *Cryst. Growth Des*. **2009**, *9*, 3676–3682.
6. Bokhimi, X.; Pedraza, F. Characterization of brookite and a new corundum-like titania phase synthesized under hydrothermal conditions. *J. Solid State Chem*. **2004**, *177*, 2456–2463.
7. Rietveld, H.M. A profile refinement method for nuclear and magnetic structures. *J. Appl. Crystallogr*. **1969**, *2*, 65–71.
8. Tompsett, G.A.; Bowmaker, G.A.; Cooney, R.P.; Metson, J.B.; Rodgers, K.A.; Seakins, J.M. The Raman spectrum of brookite, $TiO_2$ (Pbca, Z = 8). *J. Raman Spectrosc*. **1995**, *26*, 57–62.
9. Zhang, H.; Banfield, J.F. Understanding polymorphic phase transformation behavior during growth of nanocrystalline aggregates: Insights from $TiO_2$. *J. Phys. Chem.* B **2000**, *104*, 3481–3487.

10. Zhu, K.-R.; Zhang, M.-S.; Hong, J.-M.; Yin, Z. Size effect on phase transition sequence of $TiO_2$ nanocrystal. *Mater. Sci. Eng. A* **2003**, *403*, 87–93.
11. Grätzel, M.; Rotzinger, F.P. The influence of the crystal lattice structure on the conduction band energy of oxides of titanium(IV). *Chem. Phys. Lett*. **1985**, *118*, 474–477.
12. Mo, S.D.; Ching, W.Y. Electronic and optical properties of three phases of titanium dioxide: Rutile, anatase and brookite. *Phys. Rev. B* **1995**, *51*, 13023–13032.
13. Park, J.-Y.; Lee, C.; Jung, K.-W.; Jung, D. Structure related photocatalytic properties of $TiO_2$. *Bull. Korean Chem. Soc*. **2009**, *30*, 402–404.
14. Landmann, M.; Rauls, E.; Schmidt, W.G. The electronic structure and optical response of rutile, anatase and brookite $TiO_2$. *J. Phys.* **2012**, *24*, doi:10.1088/0953-8984/24/19/195503.
15. Kim, Y.I.; Atherton, S.J.; Brigham, E.S.; Mallouk, T.E. Sensitized layered metal oxide semiconductor particles for photochemical hydrogen evolution from nonsacrificial electron donors. *J. Phys. Chem*. **1993**, *97*, 11802–11810.
16. Štengl, V.; Králová, D. Photoactivity of brookite–rutile $TiO_2$ nanocrystalline mixtures obtained by heat treatment of hydrothermally prepared brookite. *Mater. Chem. Phys*. **2011**, *129*, 794–801.
17. Reyes-Coronado, D.; Rodríguez-Gattorno, G.; Espinosa-Pesqueira, M.E.; Cab, C.; de Coss, R.; Oskam, G. Phase-pure $TiO_2$ nanoparticles: Anatase, brookite and rutile. *Nanotechnology* **2008**, *19*, doi:10.1088/0957-4484/19/14/145605.
18. Xie, J.; Lü, X.; Liu, J.; Shu, H. Brookite titania photocatalytic nanomaterials: Synthesis, properties, and applications. *Pure Appl. Chem*. **2009**, *81*, 2407–2415.
19. Shen, X.; Zhang, J.; Tian, B.; Anpo, M. Tartaric acid-assisted preparation and photocatalytic performance of titania nanoparticles with controllable phases of anatase and brookite. *J. Mater. Sci*. **2012**, *47*, 5743–5751.
20. Mattsson, A.; Österlund, L. Adsorption and photoinduced decomposition of acetone and acetic acid on anatase, brookite, and rutile $TiO_2$ nanoparticles. *J. Phys. Chem. C* **2010**, *114*, 14121–14132.
21. Koelsch, M.; Cassaignon, S.; Guillemoles, J.F.; Jolivet, J.-P. Comparison of optical and electrochemical properties of anatase and brookite $TiO_2$ synthesized by the sol–gel method. *Thin Solid Films* **2002**, *403–404*, 312–319.
22. Magne, C.; Dufour, F.; Labat, F.; Lancel, G.; Durupthy, O.; Cassaignon, S.; Pauporté, T. Effects of $TiO_2$ nanoparticle polymorphism on dye-sensitized solar cell photovoltaic properties. *J. Photochem. Photobiol. A* **2012**, *232*, 22–31.
23. Kandiel, T.A.; Feldhoff, A.; Robben, L.; Dillert, R.; Bahnemann, D.W. Tailored titanium dioxide nanomaterials: Anatase nanoparticles and brookite nanorods as highly active photocatalysts. *Chem. Mater*. **2010**, *22*, 2050–2060.
24. Di Paola, A.; Cufalo, G.; Addamo, M.; Bellardita, M.; Campostrini, R.; Ischia, M.; Ceccato, R.; Palmisano, L. Photocatalytic activity of nanocrystalline $TiO_2$ (brookite, rutile and brookite-based) powders prepared by thermohydrolysis of $TiCl_4$ in aqueous chloride solutions. *Colloids Surf. A* **2008**, *317*, 366–376.
25. Nguyen-Phan, T.-D.; Kim, E.J.; Hahn, S.H.; Kim, W.-J.; Shin, E.W. Synthesis of hierarchical rose bridal bouquet- and humming-top-like $TiO_2$ nanostructures and their shape-dependent degradation efficiency of dye. *J. Colloid Interface Sci*. **2011**, *356*, 138–144.

26. Zallen, R.; Moret, M.P. The optical absorption edge of brookite $TiO_2$. *Solid State Commun*. **2006**, *137*, 154–157.
27. Lin, H.; Li, L.; Zhao, M.; Huang, X.; Chen, X.; Li, G.; Yu, R. Synthesis of high-quality brookite $TiO_2$ single-crystalline nanosheets with specific facets exposed: Tuning catalysts from inert to highly reactive. *J. Am. Chem. Soc*. **2012**, *134*, 8328–8331.
28. Shibata, T.; Irie, H.; Ohmori, M.; Nakajima, A.; Watanabe, T.; Hashimoto, K. Comparison of photochemical properties of brookite and anatase $TiO_2$ films. *Phys. Chem. Chem. Phys*. **2004**, *6*, 1359–1362.
29. Dung, D.; Ramsden, J.; Grätzel, M. Dynamics of interfacial electron-transfer processes in colloidal semiconductor systems. *J. Am. Chem. Soc*. **1982**, *104*, 2977–2985.
30. Di Paola, A.; Bellardita, M.; Ceccato, R.; Palmisano, L.; Parrino, F. Highly active photocatalytic $TiO_2$ powders obtained by thermohydrolysis of $TiCl_4$ in water. *J. Phys. Chem. C* **2009**, *113*, 15166–15174.
31. Roy, A.M.; De, G.C.; Sasmal, N.; Bhattacharyya, S.S. Determination of the flat band potential of semiconductor particles in suspension by photovoltage measurement. *Int. J. Hydrogen Energy* **1995**, *20*, 627–630.
32. Truong, Q.D.; Le, T.H.; Liu, J.-Y.; Chung, C.-C.; Ling, Y.-C. Synthesis of $TiO_2$ nanoparticles using novel titanium oxalate complex towards visible light-driven photocatalytic reduction of $CO_2$ to $CH_3OH$. *Appl. Catal. A* **2012**, *437–438*, 28–35.
33. Glemser, O.; Schwarzmann, E. Zur Polymorphie des Titandioxyds. *Angew. Chem*. **1956**, *68*, 791.
34. Knoll, H.; Kühnhold, U. Über die Stabilität des Anatas. *Naturwiss* **1957**, *44*, 394.
35. Knoll, H. Zur Bildung von Brookit. *Naturwiss* **1961**, *48*, 601.
36. Yamaguchi, S. Brookite film on titanium. *J. Electrochem. Soc*. **1961**, *108*, 302.
37. Knoll, H. Umwandlung von Anatas in Brookit. *Naturwiss* **1963**, *50*, 546.
38. Knoll, H. Darstellung von Brookit. *Angew. Chem*. **1964**, *76*, 592.
39. Keesmann, I. Zur hydrothermalen Synthese von Brookit. *Z. Anorg. Allg. Chem*. **1966**, *346*, 30–43.
40. Schwarzmann, E.; Ognibeni, K.H. Hydrothermal synthesis of brookite $TiO_2$. *Z. Naturforsch. B* **1974**, *29*, 435.
41. Kiyama, M.; Akita, T.; Tsutsumi, Y.; Takada, T. Formation of titanic oxides of anatase, brookite and rutile types by aerial oxidation of titanous solutions. *Chem. Lett*. **1972**, 21–24.
42. Ohtani, B.; Handa, J.-I.; Nishimoto, S.I.; Kagiya, T. Highly active semiconductor photocatalyst: Extra-fine crystallite of brookite $TiO_2$ for redox reaction in aqueous propan-2-ol and/or silver sulfate solution. *Chem. Phys. Lett*. **1985**, *120*, 292–294.
43. Oota, T.; Yamai, I.; Saito, H. Brookite formation by the oxidation of titanium metal under hydrothermal conditions. *J. Ceram. Soc. Jpn*. **1979**, *87*, 375–382 (in Japanese).
44. Oota, T.; Yamai, I.; Saito, H. Hydrothermal syntesis of brookite from various titanium compounds and its formation mechanism. *J. Ceram. Soc. Jpn*. **1979**, *87*, 512–519 (in Japanese).
45. Mitsuhashi, T.; Watanabe, M. Brookite formation from precipitates containing calcium ions. *Mineral J*. **1978**, *9*, 236–240.
46. Arnal, P.; Corriu, R.J.P.; Leclercq, D.; Mutin, P.H.; Vioux, A. Preparation of anatase, brookite and rutile at low temperature by non-hydrolytic sol-gel methods. *J. Mater. Chem*. **1996**, *6*, 1925–1932.

47. Nagase, T.; Ebina, T.; Iwasaki, T.; Hayashi, H.; Onodera, Y.; Chatterjee, M. Hydrothermal synthesis of brookite. *Chem. Lett*. **1999**, *28*, 911–912.
48. Kominami, H.; Kohno, M.; Kera, Y. Synthesis of brookite-type titanium oxide nano-crystals in organic media. *J. Mater. Chem*. **2000**, *10*, 1151–1156.
49. Zheng, Y.; Shi, E.; Cui, S.; Li, W.; Hu, X. Hydrothermal preparation of nanosized brookite powders. *J. Am. Ceram. Soc*. **2000**, *83*, 2634–2636.
50. Zheng, Y.; Shi, E.; Cui, S.; Li, W.; Hu, X. Hydrothermal preparation and characterization of brookite-type $TiO_2$ nanocrystallites. *J. Mater. Sci. Lett*. **2000**, *19*, 1445–1448.
51. Pottier, A.; Chanéac, C.; Tronc, E.; Mazerolles, L.; Jolivet, J.-P. Synthesis of brookite $TiO_2$ nanoparticles by thermolysis of $TiCl_4$ in strongly acidic aqueous media. *J. Mater. Chem*. **2001**, *11*, 1116–1121.
52. Di Paola, A.; Bellardita, M.; Palmisano, L. $TiO_2$ photocatalysts prepared by thermohydrolysis of $TiCl_4$ in aqueous solutions. *Stud. Surf. Sci. Catal*. **2010**, *175*, 225–228.
53. Lee, B.I.; Wang, X.; Bhave, R.; Hu, M. Synthesis of brookite $TiO_2$ nanoparticles by ambient condition sol process. *Mater. Lett*. **2006**, *60*, 1179–1183.
54. Bhave, R.C.; Lee, B.I. Experimental variables in the synthesis of brookite phase $TiO_2$ nanoparticles. *Mater. Sci. Eng. A* **2007**, *467*, 146–149.
55. Lee, J.H.; Yang, Y.S. Synthesis of $TiO_2$ nanoparticles with pure brookite at low temperature by hydrolysis of $TiCl_4$ using $HNO_3$ solution. *J. Mater. Sci*. **2006**, *41*, 557–559.
56. Cassaignon, S.; Koelsch, M.; Jolivet, J.-P. Selective synthesis of brookite, anatase and rutile nanoparticles: thermolysis of $TiCl_4$ in aqueous nitric acid. *J. Mater. Sci*. **2007**, *42*, 6689–6695.
57. Buonsanti, R.; Grillo, V.; Carlino, E.; Giannini, C.; Kipp, T.; Cingolani, R.; Cozzoli, P.D. Nonhydrolytic synthesis of high-quality anisotropically shaped brookite $TiO_2$ nanocrystals. *J. Am. Chem. Soc*. **2008**, *130*, 11223–11233.
58. Koelsch, M.; Cassaignon, S.; Ta Thanh Minh, C.; Guillemoles, J.-F.; Jolivet, J.-P. Electrochemical comparative study of titania (anatase, brookite and rutile) nanoparticles synthesized in aqueous medium. *Thin Solid Films* **2004**, *451–452*, 86–92.
59. Yang, S.-F.; Luo, W.; Zhu, Y.-C.; Liu, Y.-H.; Zhao, J.-Z.; Wang, Z.-C.; Zou, G.-T. Preparation of brookite $TiO_2$ micro-crystals with single phase. *Chem. J. Chin. Univ*. **2003**, *24*, 1933–1936 (in Chinese).
60. Zhang, J.; Yan, S.; Fu, L.; Wang, F.; Yuan, M.; Luo, G.; Xu, Q.; Wang, X.; Li, C. Photocatalytic degradation of rhodamine B on anatase, rutile, and brookite $TiO_2$. *Chin. J. Catal*. **2011**, *32*, 983–991.
61. Xu, Q.; Zhang, J.; Feng, Z.; Ma, Y.; Wang, X.; Li, C. Surface structural transformation and the phase transition kinetics of brookite $TiO_2$. *Chem. Asian J*. **2010**, *5*, 2158–2161.
62. Luo, W.; Yang, S.F.; Wang, Z.C.; Wang, Y.; Ahuja, R.; Johansson, B.; Liu, J.; Zou, G.T. Structural phase transitions in brookite-type $TiO_2$ under high pressure. *Solid State Commun*. **2005**, *133*, 49–53.
63. Dambournet, D.; Belharouak, I.; Amine, K. Tailored preparation methods of $TiO_2$ anatase, rutile, brookite: Mechanism of formation and electrochemical properties. *Chem. Mater*. **2010**, *22*, 1173–1179.
64. Dambournet, D.; Belharouak, I.; Ma, J.; Amine, K. Toward high surface area $TiO_2$ brookite with morphology control. *J. Mater. Chem*. **2011**, *21*, 3085–3090.

65. Li, J.-G.; Tang, C.; Li, D.; Haneda, H.; Ishigaki, T. Monodispersed spherical particles of brookite-type $TiO_2$: Synthesis, characterization, and photocatalytic property. *J. Am. Ceram. Soc*. **2004**, *87*, 1358–1361.
66. Bakardjieva, S.; Štengl, V.; Szatmary, L.; Subrt, J.; Lukac, J.; Murafa, N.; Niznansky, D.; Cizek, K.; Jirkovskyc, J.; Petrova, N. Transformation of brookite-type $TiO_2$ nanocrystals to rutile: Correlation between microstructure and photoactivity. *J. Mater. Chem*. **2006**, *16*, 1709–1716.
67. Štengl, V.; Bakardjieva, S.; Murafa, N.; Šubrt, J.; Měšťánková, H.; Jirkovský, J. Preparation, characterization and photocatalytic activity of optically transparent titanium dioxide particles. *Mater. Chem. Phys*. **2007**, *105*, 38–46.
68. Shen, X.; Tian, B.; Zhang, J. Tailored preparation of titania with controllable phases of anatase and brookite by an alkalescent hydrothermal route. *Catal. Today* **2013**, *201*, 151–158.
69. Inada, M.; Iwamoto, K.; Enomoto, N.; Hojo, J. Synthesis and photocatalytic activity of small brookite particles by self-hydrolysis of $TiOCl_2$. *J. Ceram. Soc. Jpn.* **2011**, *119*, 451–455.
70. Liu, C.-E.; Rouet, A.; Sutrisno, H.; Puzenat, E.; Terrisse, H.; Brohan, L.; Richard-Plouet, M. Low temperature synthesis of nanocrystallized titanium oxides with layered or tridimensional frameworks, from $[Ti_8O_{12}(H_2O)_{24}]Cl_8 \cdot HCl \cdot 7H_2O$ hydrolysis. *Chem. Mater*. **2008**, *20*, 4739–4748.
71. Deng, Q.; Wei, M.; Ding, X.; Jiang, L.; Ye, B.; Wei, K. Brookite-type $TiO_2$ nanotubes. *Chem. Commun*. **2008**, doi:10.1039/B802896F.
72. Deng, Q.; Wei, M.; Hong, Z.; Ding, X.; Jiang, L.; Wei, K. Selective synthesis of rutile, anatase and brookite nanorods by a hydrothermal route. *Curr. Nanosci*. **2010**, *6*, 479–482.
73. Murakami, N.; Kamai, T.; Tsubota, T.; Ohno, T. Novel hydrothermal preparation of pure brookite-type titanium(IV) oxide nanocrystal under strong acidic conditions. *Catal. Commun*. **2009**, *10*, 963–966.
74. Oskam, G.; de Jesús Peet Poot, F. Synthesis of ZnO and $TiO_2$ nanoparticles. *J. Sol-Gel Sci. Techn*. **2006**, *37*, 157–160.
75. Srivatsa, K.M.K.; Bera, M.; Basu, A. Pure brookite titania crystals with large surface area deposited by plasma enhanced chemical vapour deposition technique. *Thin Solid Films* **2008**, *516*, 7443–7446.
76. Hall, S.R.; Swinerd, V.M.; Newby, F.N.; Collins, A.M.; Mann, S. Fabrication of porous titania (brookite) microparticles with complex morphology by sol-gel replication of pollen grains. *Chem. Mater*. **2006**, *18*, 598–600.
77. Shi, J.; Shang, S.; Yang, L.; Yan, J. Morphology and crystalline phase-controllable synthesis of $TiO_2$ and their morphology-dependent photocatalytic properties. *J. Alloys Compd*. **2009**, *479*, 436–439.
78. Zhao, B.; Chen, F.; Huang, Q.; Zhang, J. Brookite $TiO_2$ nanoflowers. *Chem. Commun*. **2009**, 5115–5117.
79. Zhao, B.; Chen, F.; Jiao, Y.; Zhang, J. Phase transition and morphological evolution of titania/titanate nanomaterials under alkalescent hydrothermal treatment. *J. Mater. Chem*. **2010**, *20*, 7990–7997.

80. Jiao, Y.; Chen, F.; Zhao, B.; Yang, H.; Zhang, J. Anatase grain loaded brookite nanoflower hybrid with superior photocatalytic activity for organic degradation. *Colloids Surf. A* **2012**, *402*, 66–71.
81. Arıer, Ü.Ö.A.; Tepehan, F.Z. Controlling the particle size of nanobrookite $TiO_2$ thin films. *J. Alloys Compd*. **2011**, *509*, 8262–8267.
82. Zhang, L.; Menendez-Flores, V.M.; Murakami, N.; Ohno, T. Improvement of photocatalytic activity of brookite titanium dioxide nanorods by surface modification using chemical etching. *Appl. Surf. Sci*. **2012**, *238*, 5803–5809.
83. Li, J.-G.; Ishigaki, T. Brookite→rutile phase transformation of $TiO_2$ studied with monodispersed particles. *Acta Mater*. **2004**, *52*, 5143–5150.
84. Kakihana, M.; Kobayashi, M.; Tomita, K.; Petrykin, V. Application of water-soluble titanium complexes as precursors for synthesis of titanium-containing oxides via aqueous solution processes. *Bull. Chem. Soc. Jpn*. **2010**, *83*, 1285–1308.
85. Tomita, K.; Petrykin, V.; Kobayashi, M.; Shiro, M.; Yoshimura, M.; Kakihana, M. A water-soluble titanium complex for the selective synthesis of nanocrystalline brookite, rutile, and anatase by a hydrothermal method. *Angew. Chem. Int. Ed*. **2006**, *45*, 2378–2381.
86. Kobayashi, M.; Tomita, K.; Petrykin, V.; Yoshimura, M.; Kakihana, M. Direct synthesis of brookite-type titanium oxide by hydrothermal method using water-soluble titanium complexes. *J. Mater. Sci*. **2008**, *43*, 2158–2162.
87. Morishima, Y.; Kobayashi, M.; Petrykin, V.; Kakihana, M.; Tomita, K. Microwave-assisted hydrothermal synthesis of brookite nanoparticles from a water-soluble titanium complex and their photocatalytic activity. *J. Ceram. Soc. Jpn*. **2007**, *115*, 826–830.
88. Kobayashi, M.; Tomita, K.; Petrykin, V.; Yin, S.; Sato, S.; Yoshimura, M.; Kakihana, M. Hydrothermal synthesis of nanosized titania photocatalysts using novel water-soluble titanium complexes. *Solid State Phenom*. **2007**, *124–126*, 723–726.
89. Ismail, A.A.; Kandiel, T.A.; Bahnemann, D.W. Novel (and better?) titania-based photocatalysts: Brookite nanorods and mesoporous structures. *J. Photochem. Photobiol. A* **2010**, *216*, 183–193.
90. Truong, Q.D.; Kobayashi, M.; Kato, H.; Kakihana, M. Hydrothermal synthesis of hierarchical $TiO_2$ microspheres using a novel titanium complex coordinated by picolinic acid. *J. Ceram. Soc. Jpn*. **2011**, *119*, 513–516.
91. Morishima, Y.; Kobayashi, M.; Petrykin, V.; Yin, S.; Sato, T.; Kakihana, M.; Tomita, K. Hydrothermal synthesis of brookite type $TiO_2$ photocatalysts using a water-soluble Ti-complex coordinated by ethilenediaminetetraacetic. *J. Ceram. Soc. Jpn*. **2009**, *117*, 320–325.
92. Ozawa, T.C.; Sasaki, T. An alkali-metal ion extracted layered compound as a template for a metastable phase synthesis in a low-temperature solid-state reaction: preparation of brookite from $K_{0.8}Ti_{1.73}Li_{0.27}O_4$. *Inorg. Chem*. **2010**, *49*, 3044–3050.
93. Wakamatsu, T.; Fujiwara, T.; Ishihara, K.N.; Shingu, P.H. Formation of brookite-type $TiO_2$ titania by mechanical alloying. *J. Jpn. Soc. Powder Powder Metall*. **2001**, *48*, 950–954.
94. Perego, C.; Wang, Y.-H.; Durupthy, O.; Cassaignon, S.; Revel, R.; Jolivet, J.-P. Nanocrystalline brookite with enhanced stability and photocatalytic activity: influence of lanthanum(III) doping. *ACS Appl. Mater. Interfaces* **2012**, *4*, 752–760.

95. Ohno, Y.; Tomita, K.; Komatsubara, Y.; Taniguchi, T.; Katsumata, K.; Matsushita, N.; Kogure, T.; Okada, K. Pseudo-cube shaped brookite ($TiO_2$) nanocrystals synthesized by an oleate-modified hydrothermal growth method. *Cryst. Growth Des*. **2011**, *11*, 4831–4836.
96. Iskandar, F.; Nandiyanto, A.B.D.; Yun, K.M.; Hogan, C.J., Jr.; Okuyama, K.; Biswas, P. Enhanced photocatalytic performance of brookite $TiO_2$ macroporous particles prepared by spray drying with colloidal templating. *Adv. Mater*. **2007**, *19*, 1408–1412.
97. Katagiri, K.; Inami, H.; Koumoto, K.; Inumaru, K.; Tomita, K.; Kobayashi, M.; Kakihana, M. Preparation of hollow $TiO_2$ spheres of the desired polymorphs by layer-by-layer assembly of a water-soluble titanium complex and hydrothermal treatment. *Eur. J. Inorg. Chem*. **2012**, *2012*, 3267–3272.
98. Takahashi, Y.; Wakayama, S.; Ogiso, A.; Sugiyama, K. Selective deposition of anatase, rutile and brookite films by vapour phase decomposition of alkyl titanates. *Kinzoko Hyomen Gijutsu* **1984**, *35*, 584–589 (in Japanese).
99. Arsov, L.D.; Kormann, C.; Plieth, W. *In situ* Raman spectra of anodically formed titanium dioxide layers in solutions of $H_2SO_4$, KOH, and $HNO_3$. *J. Electrochem. Soc*. **1991**, *138*, 2964–2970.
100. Arsov, L.D.; Kormann, C.; Plieth, W. Electrochemical synthesis and *in situ* Raman spectroscopy of thin films of titanium dioxide. *J. Raman Spectrosc*. **1991**, *22*, 573–575.
101. Moret, M.P.; Zallen, R.; Vijay, D.P.; Desu, S.B. Brookite-rich titania films made by pulsed laser deposition. *Thin Solid Films* **2000**, *366*, 8–10.
102. Djaoued, Y.; Brüning, R.; Bersani, D.; Lottici, P.P.; Badilescu, S. Sol–gel nanocrystalline brookite-rich titania films. *Mater. Lett*. **2004**, *58*, 2618–2622.
103. Jiang, K.-J.; Kitamura, T.; Yin, H.; Ito, S.; Yanagida, S. Dye-sensitized solar cells using brookite nanoparticle $TiO_2$ films as electrodes. *Chem. Lett*. **2002**, *31*, 872–873.
104. Ohara, C.; Hongo, T.; Yamazaki, A.; Nagoya, T. Synthesis and characterization of brookite/anatase complex thin film. *Appl. Surf. Sci*. **2008**, *254*, 6619–6622.
105. Pan, H.; Qiu, X.; Ivanov, I.N.; Meyer, H.M.; Wang, W.; Zhu, W.; Paranthaman, M.P.; Zhang, Z.; Eres, G.; Gu, B. Fabrication and characterization of brookite-rich, visible light-active $TiO_2$ films for water splitting. *Appl. Catal. B* **2009**, *93*, 90–95.
106. Bach, H.; Schroeder, H. Kristallstruktur und optische eigenschaften von dünnen organogenen titanoxyd-schichten auf glasunterlagen. *Thin Solid Films* **1968**, *1*, 255–276.
107. López, A.; Acosta, D.; Martínez, A.I.; Santiago, J. Nanostructured low crystallized titanium dioxide thin films with good photocatalytic activity. *Powder Technol*. **2010**, *202*, 111–117.
108. Novotna, P.; Krysa, J.; Maixner, J.; Kluson, P.; Novak, P. Photocatalytic activity of sol–gel $TiO_2$ thin films deposited on soda lime glass and soda lime glass precoated with a $SiO_2$ layer. *Surf. Coat. Technol*. **2010**, *204*, 2570–2575.
109. Krýsa, J.; Novotná, P.; Kment, Š.; Mills, A. Effect of glass substrate and deposition technique on the properties of sol gel $TiO_2$ thin films. *J. Photochem. Photobiol. A* **2011**, *222*, 81–86.
110. Addamo, M.; Bellardita, M.; Di Paola, A.; Palmisano, L. Preparation and photoactivity of nanostructured anatase, rutile and brookite $TiO_2$ thin films. *Chem. Commun*. **2006**, doi:10.1039/B612172A.
111. Di Paola, A.; Addamo, M.; Bellardita, M.; Cazzanelli, E.; Palmisano, L. Preparation of photocatalytic brookite thin films. *Thin Solid Films* **2007**, *515*, 3527–3529.

112. Di Paola, A.; Addamo, M.; Bellardita, M.; García-López, E.; Marcì, G.; Palmisano, L. Preparation of photocatalytic nanostructured $TiO_2$ thin films. *Mater. Sci. Forum* **2008**, *587–588*, 795–799.
113. Magne, C.; Cassaignon, S.; Lancel, G.; Pauporté, T. Brookite $TiO_2$ nanoparticle films for dye-sensitized solar cells. *ChemPhysChem* **2011**, *12*, 2461–2467.
114. Kim, S.-J.; Lee, K.; Kim, J.H.; Lee, N.-H.; Kim, S.-J. Preparation of brookite phase $TiO_2$ colloidal sol for thin film coating. *Mater. Lett*. **2006**, *60*, 364–367.
115. Caricato, A.P.; Buonsanti, R.; Catalano, M.; Cesaria, M.; Cozzoli, P.D.; Luches, A.; Manera, M.G.; Martino, M.; Taurino, A.; Rella, R. Films of brookite $TiO_2$ nanorods/nanoparticles deposited by matrix-assisted pulsed laser evaporation as $NO_2$ gas-sensing layers. *Appl. Phys. A* **2011**, *104*, 963–968.
116. Manera, M.G.; Taurino, A.; Catalano, M.; Rella, R.; Caricato, A.P.; Buonsanti, R.; Cozzoli, P.D.; Martino, M. Enhancement of the optically activated $NO_2$ gas sensing response of brookite $TiO_2$ nanorods/nanoparticles thin films deposited by matrix-assisted pulsed-laser evaporation. *Sens. Actuators B* **2012**, *161*, 869–879.
117. Li, W.-K.; Gong, X.-Q.; Lu, G.; Selloni, A. Different reactivities of $TiO_2$ polymorphs: comparative DFT calculations of water and formic acid adsorption at anatase and brookite $TiO_2$ surfaces. *J. Phys. Chem. C* **2008**, *112*, 6594–6596.
118. Kominami, H.; Ishii, Y.; Kohno, M.; Konishi, S.; Kera, Y.; Ohtani, B. Nanocrystalline brookite-type titanium(IV) oxide photocatalysts prepared by a solvothermal method: correlation between their physical properties and photocatalytic activities. *Catal. Lett*. **2003**, *91*, 41–47.
119. Kominami, H.; Kato, J.; Murakami, S.; Ishii, Y.; Kohno, M.; Yabutani, K.; Yamamoto, T.; Kera, Y.; Inoue, M.; Inui, T.; Ohtani, B. Solvothermal syntheses of semiconductor photocatalysts of ultra-high activities. *Catal. Today* **2003**, *84*, 181–189.
120. Zhou, L.-J.; Yan, S.-S.; Tian, B.-Z.; Chen, F.; Zhang, J.-L.; Huang, J.-Z.; Zhang, L.-Z. Preparation and characterization of anatase-brookite $TiO_2$ film on the PET surface. *Acta Phys. Chim. Sin.* **2006**, *22*, 569–573 (in Chinese).
121. Bellardita, M.; Di Paola, A.; Palmisano, L.; Parrino, F.; Buscarino, G.; Amadelli, R. Preparation and photoactivity of samarium loaded anatase, brookite and rutile catalysts. *Appl. Catal. B* **2011**, *104*, 291–299.
122. Yin, S.; Ihara, K.; Liu, B.; Wang, Y.; Li, R.; Sato, T. Preparation of anatase, rutile and brookite type anion doped titania photocatalyst nanoparticles and thin films. *Phys. Scr.* **2007**, *T129*, 268–273.
123. Chiarello, G.L.; Di Paola, A.; Palmisano, L.; Selli, E. Effect of titanium dioxide crystalline structure on the photocatalytic production of hydrogen. *Photochem. Photobiol. Sci*. **2011**, *10*, 355–360.
124. Lee, B.I.; Kaewgun, S.; Kim, W.; Choi, W.; Lee, J.S.; Kim, E. Visible light photocatalytic properties of polymorphic brookite titania. *J. Renew. Sustain. Energy* **2009**, *1*, 023101.
125. Anji Reddy, M.; Satya Kishore, M.; Pralong, V.; Varadaradju, U.V.; Raveau, B. Lithium intercalation into nanocrystalline brookite $TiO_2$. *Electrochem. Solid-State Lett*. **2007**, *10*, A29–A31.
126. Anji Reddy, M.; Pralong, V.; Varadaradju, U.V.; Raveau, B. Crystallite size constraints on lithium insertion into brookite $TiO_2$. *Electrochem. Solid State Lett*. **2008**, *11*, A132–A134.

127. Lee, D.-H.; Park, J.-G.; Choi, K.J.; Choi, H.-J.; Kim, D.-W. Preparation of brookite-type $TiO_2$/carbon nanocomposite electrodes for application to Li ion batteries. *Eur. J. Inorg. Chem*. **2008**, *2008*, 878–882.
128. Lee, D.-H.; Kim, D.-W.; Park, J.-G. Enhanced rate capabilities of nanobrookite with electronically conducting MWCNT networks. *Cryst. Growth Des*. **2008**, *8*, 4506–4510.
129. Ohtani, B.; Kawaguchi, J.; Kozawa, M.; Nakaoka, Y.; Nosaka, Y.; Nishimoto, S. Effect of platinum loading on the photocatalytic activity of cadmium(II) sulfide particles suspended in aqueous amino acid solutions. *J. Photochem. Photobiol. A* **1995**, *90*, 75–80.
130. Maldotti, A.; Amadelli, R.; Samiolo, L.; Molinari, A.; Penoni, A.; Tollari, S.; Cenini, S. Photocatalytic formation of a carbamate through ethanol-assisted carbonylation of *p*-nitrotoluene. *Chem. Commun*. **2005**, 1749–1751.
131. Addamo, M.; Augugliaro, V.; Bellardita, M.; Di Paola, A.; Loddo, V.; Palmisano, G.; Palmisano, L.; Yurdakal, S. Environmentally friendly photocatalytic oxidation of aromatic alcohol to aldehyde in aqueous suspension of brookite $TiO_2$. *Catal. Lett*. **2008**, *126*, 58–62.
132. Augugliaro, V.; Loddo, V.; López-Muñoz, M.J.; Márquez-Álvarez, C.; Palmisano, G.; Palmisano, L.; Yurdakal, S. Home-prepared anatase, rutile, and brookite $TiO_2$ for selective photocatalytic oxidation of 4-methoxybenzyl alcohol in water: reactivity and ATR-FTIR study. *Photochem. Photobiol. Sci*. **2009**, *8*, 663–669.
133. Palmisano, L.; Augugliaro, V.; Bellardita, M.; Di Paola, A.; García López, E.; Loddo, V.; Marcì, G.; Palmisano, G.; Yurdakal, S. Titania photocatalysts for selective oxidations in water. *ChemSusChem* **2011**, *4*, 1431–1438.
134. Liu, L.; Zhao, H.; Andino, J.M.; Li, Y. Photocatalytic $CO_2$ reduction with $H_2O$ on $TiO_2$ nanocrystals: Comparison of anatase, rutile, and brookite polymorphs and exploration of surface chemistry. *ACS Catal.* **2012**, *2*, 1817–1828.
135. Asahi, R.; Morikawa, T.; Ohwaki, T.; Aoki, K.; Taga, Y. Visible-light photocatalysis in nitrogen-doped titanium oxides. *Science* **2001**, *293*, 269–271.
136. Aita, Y.; Komatsu, M.; Yin, S.; Sato, T. Phase-compositional control and visible light photocatalytic activity of nitrogen-doped titania via solvothermal process. *J. Solid State Chem*. **2004**, *177*, 3235–3238.
137. Yin, S.; Aita, Y.; Komatsu, M.; Wang, J.; Tang, Q.; Sato, T. Synthesis of excellent visible-light responsive $TiO_{2-x}N_y$ photocatalyst by a homogeneous precipitation-solvothermal process. *J. Mater. Chem*. **2005**, *15*, 674–682.
138. Sato, T.; Aita, Y.; Komatsu, M.; Yin, S. Solvothermal synthesis of visible light responsive nitrogen-doped titania nanocrystals. *J. Mater. Sci*. **2006**, *41*, 1433–1438.
139. Bonsu, P.O.; Lü, X.; Xie, J.; Jiang, D.; Chen, M.; Wei, X. Photoenhanced degradation of rhodamine blue on monometallic gold (Au) loaded brookite titania photocatalysts activated by visible light. *React. Kinet. Mech. Catal*. **2012**, *107*, 487–502.
140. Yan, W.; Chen, B.; Mahurin, S.M.; Dai, S.; Overbury, S.H. Brookite-supported highly stable gold catalytic system for CO oxidation. *Chem. Commun*. **2004**, doi:10.1039/B405434B.
141. Ranjit, K.T.; Cohen, H.; Willer, I.; Bossmann, S.; Braun, A.M. Lanthanide oxide-doped titanium dioxide: effective photocatalysts for the degradation of organic pollutants. *J. Mater. Sci*. **1999**, *34*, 5273–5280.

142. Ranjit, K.T.; Willer, I.; Bossmann, S.; Braun, A.M. Lanthanide oxide-doped titanium dioxide photocatalysts: Novel photocatalysts for the enhanced degradation of *p*-chlorophenoxyacetic acid. *Environ. Sci. Technol*. **2001**, *35*, 1544–1549.
143. Bellardita, M.; Di Paola, A.; Palmisano, L.; Parrino, F.; Buscarino, G.; Amadelli, R. Preparation of Sm-loaded brookite $TiO_2$ photocatalysts. *Catal. Today* **2011**, *161*, 35–40.
144. Luca, D.; Mardare, D.; Iacomi, F.; Teodorescu, C.M. Increasing surface hydrophilicity of titania films by doping. *Appl. Surf. Sci*. **2006**, *252*, 6122–6126.
145. Eshaghi, A.; Eshaghi, A. Optical and hydrophilic properties of nanostructure Cu loaded brookite $TiO_2$ thin film. *Thin Solid Films* **2011**, *520*, 1053–1056.
146. Lü, X.; Liu, J.; Zhang, H.; Ding, J.; Xie, J. Structure and property of mesoporous molybdenum/carbon co-doped brookite titania. *Trans. Nonferrous Met. Soc. China* **2009**, *19*, 669–673.
147. Hotchandani, S.; Kamat, P.V. Charge-transfer processes in coupled semiconductor systems. Photochemistry and photoelectrochemistry of the colloidal CdS-ZnO system. *J. Phys. Chem*. **1992**, *96*, 6834–6839.
148. Serpone, N.; Maruthamuthu, P.; Pichat, P.; Pelizzetti, E.; Hidaka, H. Exploiting the interparticle electron transfer process in the photocatalysed oxidation of phenol, 2-chlorophenol and pentachlorophenol: Chemical evidence for electron and hole transfer between coupled semiconductors. *J. Photochem. Photobiol. A* **1995**, *85*, 247–255.
149. Di Paola, A.; Palmisano, L.; Derrigo, M.; Augugliaro, V. Preparation and characterization of tungsten chalcogenide photocatalysts. *J. Phys. Chem. B* **1997**, *101*, 876–883.
150. Ovenstone, J. Preparation of novel titania photocatalysts with high activity. *J. Mater. Sci.* **2001**, *36*, 1325–1329.
151. Li, Y.; Lee, N.-H.; Hwang, D.-S.; Song, J.S.; Lee, E.G.; Kim, S.-J. Synthesis and characterization of nano titania powder with high photoactivity for gas-phase photo-oxidation of benzene from $TiOCl_2$ aqueous solution at low temperatures. *Langmuir* **2004**, *20*, 10838–10844.
152. Li, Y.; Lee, N.-H.; Song, J.S.; Lee, E.G.; Kim, S.-J. Synthesis and photocatalytic properties of nano bi-crystalline titania of anatase and brookite by hydrolyzing $TiOCl_2$ aqueous solution at low temperatures. *Res. Chem. Intermed*. **2005**, *31*, 309–318.
153. Yu, J.C.; Yu, J.; Ho, W.; Zhang, L. Preparation of highly photocatalytic active nano-sized $TiO_2$ particles via ultrasonic irradiation. *Chem. Commun*. **2001**, doi:10.1039/B105471F.
154. Yu, J.; Yu, J.C.; Leung, M.K.-P.; Ho, W.; Cheng, B.; Zhao, X.; Zhao, J. Effects of acidic and basic hydrolysis catalysts on the photocatalytic activity and microstructures of bimodal mesoporous titania. *J. Catal*. **2003**, *217*, 69–78.
155. Yu, J.C.; Yu, J.; Zhang, L.; Ho, W. Enhancing effects of water content and ultrasonic irradiation on the photocatalytic activity of nano-sized $TiO_2$ powders. *J. Photochem. Photobiol. A* **2002**, *148*, 263–271.
156. Yu, J.C.; Zhang, L.; Yu, J. Direct sonochemical preparation and characterization of highly active mesoporous $TiO_2$ with a bicrystalline framework. *Chem. Mater*. **2002**, *14*, 4647–4653.
157. Ozawa, T.; Iwasaki, M.; Tada, H.; Akita, T.; Tanaka, K.; Ito, S. Low-temperature synthesis of anatase–brookite composite nanocrystals: The junction effect on photocatalytic activity. *J. Colloid Interface Sci*. **2005**, *281*, 510–513.

158. Perera, S.; Gillan, E.G. A facile solvothermal route to photocatalytically active nanocrystalline anatase $TiO_2$ from peroxide precursors. *Solid State Sci*. **2008**, *10*, 864–872.
159. Tian, G.; Fu, H.; Jing, L.; Xin, B.; Pan, K. Preparation and characterization of stable biphase $TiO_2$ photocatalyst with high crystallinity, large surface area, and enhanced photoactivity. *J. Phys. Chem. C* **2008**, *112*, 3083–3089.
160. Dufour, F.; Cassaignon, S.; Durupthy, O.; Colbeau-Justin, C.; Chanéac, C. Do $TiO_2$ nanoparticles really taste better when cooked in a microwave oven? *Eur. J. Inorg. Chem*. **2012**, *2012*, 2707–2715.
161. Lee, S.C.; Lee, H.U.; Lee, S.M.; Lee, G.; Hong, W.G.; Lee, J.; Kim, H.J. Preparation and characterization of bicrystalline $TiO_2$ photocatalysts with high crystallinity and large surface area. *Mater. Lett*. **2012**, *79*, 191–194.
162. Boppella, R.; Basak, P.; Manorama, S.V. Viable method for the synthesis of biphasic $TiO_2$ nanocrystals with tunable phase composition and enabled visible-light photocatalytic performance. *ACS Appl. Mater. Interfaces* **2012**, *4*, 1239–1246.
163. Carrera, R.; Vázquez, A.L.; Castillo, S.; Arce, E. Photocatalytic degradation of acetaldehyde by sol-gel $TiO_2$ nanoparticles: effect of the physicochemical properties on the photocatalytic activity. *Mater. Sci. Forum* **2011**, *691*, 92–98.
164. Yu, J.; Su, Y.; Cheng, B.; Zhou, M. Effects of pH on the microstructures and photocatalytic activity of mesoporous nanocrystalline titania powders prepared via hydrothermal method. *J. Mol. Catal. A* **2006**, *258*, 104–112.
165. Liu, A.R.; Wang, S.M.; Zhao, Y.R.; Zheng, Z. Low-temperature preparation of nanocrystalline $TiO_2$ photocatalyst with a very large specific surface area. *Mater. Chem. Phys*. **2006**, *99*, 131–134.
166. Zhang, Y.; Wu, L.; Zeng, Q.; Zhi, J. An approach for controllable synthesis of different-phase titanium dioxide nanocomposites with peroxotitanium complex as precursor. *J. Phys. Chem. C* **2008**, *112*, 16457–16462.
167. Qin, W.; Liu, J.-J.; Zuo, S.-L.; Yu, Y.-C.; Hao, Z.-P. Solvothermal synthesis of nanosized $TiO_2$ particles with different crystal structures and their photocatalytic activities. *J. Inorg. Mater*. **2007**, *22*, 931–936 (In Chinese).
168. Ardizzone, S.; Bianchi, C.L.; Cappelletti, G.; Gialanella, S.; Pirola, C.; Ragaini, V. Tailored anatase/brookite nanocrystalline $TiO_2$. The optimal particle features for liquid and gas-phase photocatalytic reactions. *J. Phys. Chem. C* **2007**, *111*, 13222–13231.
169. Cappelletti, G.; Bianchi, C.L.; Ardizzone, S. Nano-titania assisted photoreduction of Cr(VI). The role of the different $TiO_2$ polymorphs. *Appl. Catal. B* **2008**, *78*, 193–201.
170. Ardizzone, S.; Bianchi, C.L.; Cappelletti, G.; Naldoni, A.; Pirola, C. Photocatalytic degradation of toluene in the gas phase: Relationship between surface species and catalyst features. *Environ. Sci. Technol*. **2008**, *42*, 6671–6676.
171. Hao, H.; Zhang, J. Low temperature synthesis of crystalline mesoporous titania with high photocatalytic activity by post-treatment in nitric acid ethanol solution. *Mater. Lett*. **2009**, *63*, 106–108.
172. Zheng, R.; Meng, X.; Tang, F. Synthesis, characterization and photodegradation study of mixed-phase titania hollow submicrospheres with rough surface. *Appl. Surf. Sci*. **2009**, *255*, 5989–5994.

173. Mahdjoub, N.; Allen, N.; Kelly, P.; Vishnyakov, V. Thermally induced phase and photocatalytic activity evolution of polymorphous titania. *J. Photochem. Photobiol. A* **2010**, *210*, 125–129.
174. Nolph, C.A.; Sievers, D.E.; Kaewgun, S.; Kucera, C.J.; McKinney, D.H.; Rientjes, J.P.; White, J.L.; Bhave, R.; Lee, B.I. Photocatalytic study of polymorphic titania synthesized by ambient condition sol process. *Catal. Lett*. **2007**, *117*, 102–106.
175. Kaewgun, S.; Nolph, C.A.; Lee, B.I. Enhancing photocatalytic activity of polymorphic titania nanoparticles by NMP solvent-based ambient condition process. *Catal. Lett.* **2008**, *123*, 173–180.
176. Kaewgun, S.; Mckinney, D.; White, J.; Smith, A.; Tinker, M.; Ziska, J.; Lee, B.I. Study of visible light photocatalytic activity achieved by NMP solvent treatment of polymorphic titania. *J. Photochem. Photobiol. A* **2009**, *202*, 154–158.
177. Kaewgun, S.; Nolph, C.A.; Lee, B.I.; Wang, L.-Q. Influence of hydroxyl contents on photocatalytic activities of polymorphic titania nanoparticles. *Mater. Chem. Phys*. **2009**, *114*, 439–445.
178. Tzikalos, N.; Belessi, V.; Lambropoulou, D. Photocatalytic degradation of Reactive Red 195 using anatase/brookite $TiO_2$ mesoporous nanoparticles: optimization using response surface methodology (RSM) and kinetics studies. *Environ. Sci. Pollut. Res*. **2012**, doi: 10.1007/s11356–012–1106–7.
179. Zhang, Y.; Gan, H.; Zhang, G. A novel mixed-phase $TiO_2$/kaolinite composites and their photocatalytic activity for degradation of organic contaminants. *Chem. Eng. J*. **2011**, *172*, 936–943.
180. Ohtani, B. Preparing articles on photocatalysis–beyond the illusions, misconceptions, and speculation. *Chem. Lett*. **2008**, *37*, 217–229.
181. Prieto-Mahaney, O.O.; Murakami, N.; Abe, R.; Ohtani, B. Correlation between photocatalytic activities and structural and physical properties of titanium(IV) oxide powders. *Chem. Lett*. **2009**, *38*, 238–239.
182. Yu, Y.; Xu, D. Single-crystalline $TiO_2$ nanorods: Highly active and easily recycled photocatalysts. *Appl. Catal. B* **2007**, *73*, 166–171.
183. Xu, H.; Zhang, L. Controllable one-pot synthesis and enhanced photocatalytic activity of mixed-phase $TiO_2$ nanocrystals with tunable brookite/rutile ratios. *J. Phys. Chem. C* **2009**, *113*, 1785–1790.
184. Lopez, T.; Gomez R.; Sanchez, E.; Tzompantzi, F.; Vera, L. Photocatalytic activity in the 2,4-dinitroaniline decomposition over $TiO_2$ sol-gel derived catalysts. *J. Sol-Gel Sci. Technol*. **2001**, *22*, 99–107.
185. Zhang, J.; Xiao, X.; Nan, J. Hydrothermal-hydrolysis synthesis and photocatalytic properties of nano-$TiO_2$ with an adjustable crystalline structure. *J. Hazard. Mater*. **2010**, *176*, 617–622.
186. Tseng, Y.-H.; Kuo, C.-S.; Huang, C.-H.; Li, Y.-Y.; Chou, P.-W.; Cheng, C.-L.; Wong, M.-S. Visible-light-responsive nano-$TiO_2$ with mixed crystal lattice and its photocatalytic activity. *Nanotechnology* **2006**, *17*, 2490–2497.
187. Luís, A.M.; Neves, M.C.; Mendonça, M.H.; Monteiro, O.C. Influence of calcination parameters on the $TiO_2$ photocatalytic properties. *Mater. Chem. Phys*. **2011**, *125*, 20–25.
188. Liao, Y.; Que, W.; Jia, Q.; He, Y.; Zhang, J.; Zhong, P. Controllable synthesis of brookite/anatase/rutile $TiO_2$ nanocomposites and single-crystalline rutile nanorods array. *J. Mater. Chem*. **2012**, *22*, 7937–7944.

189. Liu, J.; Qin, W.; Zuo, S.; Yu, Y.; Hao, Z. Solvothermal-induced phase transition and visible photocatalytic activity of nitrogen-doped titania. *J. Hazard. Mater*. **2009**, *163*, 273–278.
190. Shao, G.-S.; Zhang, X.-J.; Yuan, Z.-Y. Preparation and photocatalytic activity of hierarchically mesoporous-macroporous $TiO_{2-x}N_x$. *Appl. Catal. B* **2008**, *82*, 208–218.
191. Li, L.; Liu, C.-Y. Facile synthesis of anatase–brookite mixed-phase N-doped $TiO_2$ nanoparticles with high visible-light photocatalytic activity. *Eur. J. Inorg. Chem*. **2009**, *2009*, 3727–3733.
192. Pap, Z.; Baia, L.; Mogyorósi, K.; Dombi, A.; Oszkó, A.; Danciu, V. Correlating the visible light photoactivity of N-doped $TiO_2$ with brookite particle size and bridged-nitro surface species. *Catal. Commun*. **2012**, *17*, 1–7.
193. Popa, M.; Diamandescu, L.; Vasiliu, F.; Teodorescu, C.M.; Cosoveanu, V.; Baia, M.; Feder, M.; Baia, L.; Danciu, V. Synthesis, structural characterization, and photocatalytic properties of iron-doped $TiO_2$ aerogels. *J. Mater. Sci*. **2009**, *44*, 358–364.
194. Hao, H.; Zhang, J. The study of iron (III) and nitrogen co-doped mesoporous $TiO_2$ photocatalysts: Synthesis, characterization and activity. *Microporous Mesoporous Mater*. **2009**, *121*, 52–57.
195. Yu, J.C.; Yu, J.; Ho, W.; Jiang, Z.; Zhang, L. Effects of F-doping on the photocatalytic activity and microstructures of nanocrystalline $TiO_2$ powders. *Chem. Mater*. **2002**, *14*, 3808–3816.
196. Zhang, Q.; Li, Y.; Ackerman, E.A.; Gajdardziska-Josifovska, M.; Li, H. Visible light responsive iodine-doped $TiO_2$ for photocatalytic reduction of $CO_2$ to fuels. *Appl. Catal. A* **2011**, *400*, 195–202.
197. Zhao, B.; Chen, F.; Jiao, Y.; Yang, H.; Zhang, J. $Ag_0$-loaded brookite/anatase composite with enhanced photocatalytic performance towards the degradation of methyl orange. *J. Mol. Catal. A* **2011**, *348*, 114–119.
198. Yu, J.; Xiong, J.; Cheng, B.; Liu, S. Fabrication and characterization of Ag–$TiO_2$ multiphase nanocomposite thin films with enhanced photocatalytic activity. *Appl. Catal. B* **2005**, *60*, 211–221.
199. Li, X.; Wang, L.; Lu, X. Preparation of silver-modified $TiO_2$ via microwave-assisted method and its photocatalytic activity for toluene degradation. *J. Hazard. Mater*. **2010**, *177*, 639–647.
200. Nassoko, D.; Li, Y.-F.; Li, J.-L.; Li, X.; Yu, Y. Neodymium-doped $TiO_2$ with anatase and brookite two phases: Mechanism for photocatalytic activity enhancement under visible light and the role of electron. *Int. J. Photoenergy* **2012**, Article ID 716087.